学位論文（要約）

Architecture of Functional π-Conjugated Coordination Nanosheets

of Nickel with Mixed Ligating Groups at Interfaces

（界面を駆使した複数の配位性官能基を持つ機能性π共役

ニッケル錯体ナノシートの構築）

平成29年07月 博士(理学)申請

東京大学大学院理学系研究科 化学専攻

Sun Xinsen

孫 欣森

Abstract

The unique physical and chemical properties of coordination nanosheets (CONASHs) are of immense research interest. Whereas, the construction of well-defined 2D materials and expansion of their variety remain as challenging research targets. Coordination nanosheets (CONASHs) can be constructed by bottom-up methods using the complexation reactions of metal ions with organic bridging ligands under ambient conditions. This allows their chemical structures and properties to be precisely tuned and engineered. A series of study in this thesis describe Architecture of functional π–Conjugated Coordination Nanosheets of Nickel with Mixed Ligating Groups.

In **Chapter 1**, general research concept and focus of background are discussed.

In **Chapter 2**, a π–conjugated coordination nanosheet (CONASH) comprising bis(iminothiolato)nickel moieties, **NiIT**, is ascribed. Spectroscopic results confirmed coordination motifs. Microscopic observations of **NiIT** revealed the uniform and flat nature of nanosheet. SAED analysis indicated a formation of two-dimensional hexagonal crystal structure.

In **Chapter 3**, another π–conjugated CONASH comprising bis(aminothiolato)nickel moieties, **NiAT**, is described. The morphology, composition, and crystal structure of **NiAT** were characterized by AFM, FE-SEM, XPS, ATR-IR, HR-TEM, and GIXD.

Chapter 4 further expands the topic among **NiIT** and **NiAT** utilization for electro functions. **NiAT** is an insulator and interconvertible to the conducting **NiIT** nanosheet by a proton-coupled redox reaction. These drastic changes in electrical conductivity are explained by the theoretical calculations. Both **NiIT** and **NiAT** showed remarkable performance as electrochemical HER catalysts.

In **Chapter 5**, different approaches of crystalline π–conjugated CONASH comprising bis(iminophenolato)nickel moieties, **NiIP**, with different morphological structure are described.

In **Chapter 6**, I state the summary of this series of researches.

Contents

Chapter 1 General Introduction and Research Background

1-1 Dimensionality of nanomaterials

1-1-1 Overview of low-dimensional materials

Dimensionality of materials operates an important role for the production of new materials and engendering unique physical properties. Recently low-dimensional (LD) nanomaterials have attracted much interest in the field of materials science. Low-dimensional nanomaterials represent substances of which size in particular dimensions are not over one micrometer. Their structures lead to unique physical properties which are not observed in single molecules or bulk materials. An indicative example of LD nanomaterials is a group of structurally defined carbon materials: carbon quantum dots,[1] carbon nanotubes,[2] graphenes,[3] and fullerenes,[4] as zero-, one-, two-, and three-dimensional (0D, 1D, 2D and 3D) nanomaterials (Fig. 1-1). Depending on the dimensionality, these carbon nanomaterials possess discrete chemical and physical properties as well as distinct structures. Carbon nanotube and graphene particularly have novel mechanical, electronic, optical, and chemical features deriving from the property of delocalized electrons in the specific dimensions. For example, the van Hove manners are observed among 1D carbon nanotube.[2] In comparison, graphene, a single-layer of carbon atoms arranged in a honeycomb lattice, has unique electronic performance on its 2D structure.

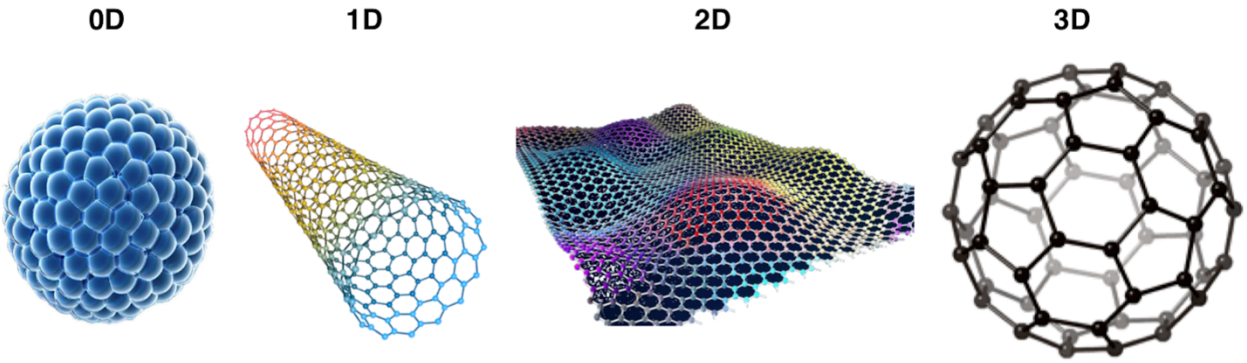

Fig. 1-1 | Dimensionality of nanomaterials. Structures of carbon quantum dots (left 1), carbon nanotube (left 2), graphene (right 2), and fullerene (right 1) work as 0D, 1D, 2D and 3D carbon nanomaterials.

1-1-2 Low-dimensional metal compounds

Metal involved chemistry is a fundamental field of chemistry and can be employed for the precise construction of various complexes for different purposes. Using metals as nodes, and organic ligands or atoms as bridges, it can result in different materials such as bulk clusters, wired-structures, films and bulk crystals (Fig. 1-2).[5-7]

As the properties of the resultant compounds can be tuned via the different combination of various metals and bridging components, researches of characteristics and relativities stemmed from electronic interactions among metals are constantly investigated vigorously. Along with the accumulation of interests among the nano-science and rapid development of microscopic techniques, scientists deeply realized that metal compounds grafting into different structures could reveal special features. However, fully adapt the chemical advantages of metal compounds into well-defined regulated structure remains a big challenge, due to the nature of metal-metal interactions and coordination bonds' lack of flexibility. Therefore, low-dimensional nanomaterials constructed by metal compounds such as nanoparticles usually confined to their stable structures, and cannot further develop to various of forms. Especially, to adapt the features of metal compounds into two-dimensional nanosheet, since the fabrication methods and structural confirmation approaches are still not developed adequately.

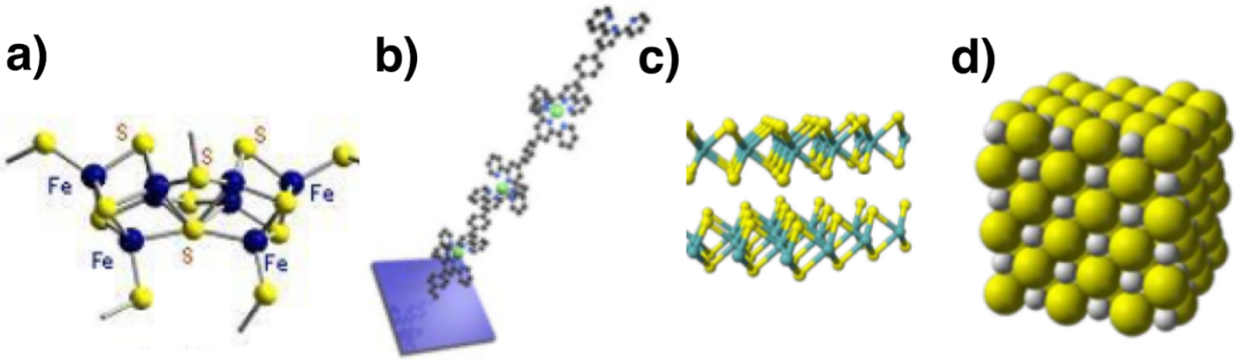

Fig. 1-2 | Dimensionality of metal compound material. Indications of 0D, 1D, 2D and 3D metal compounds.

1-2 Two-dimensional materials

1-2-1 General overview of two-dimensional materials

Two-dimensional materials are classified as materials with a film like structure and thickness of nano-order. Such nanomaterials are often regarded as nanosheet recently. This well-defined structure leads to unique physical and chemical features. For instance, in the two-dimensional structure, the carriers are restricted in a potential such that their motion in one direction is limited and thus is quantized, leaving only a two-dimensional momentum which characterises proposal in a plane normal to the confining potential.

Graphene and inorganic nanosheets are notable examples, and the anticipated potential success of graphene has prompted researchers to investigate other types of two-dimensional nanosheets.

1-2-2 Graphene and its derivatives

The advanced achievement of Novoselov and his co-authors attested that graphene,[3] a single-layered of carbon atoms regulated in a honeycomb structure, is not only a lateral stable crystal but also has excellent features including large electron and hole concentrations and great room-temperature electron mobilities. Graphene is truly the building block of a variety of carbon-based nanomaterials counting fullerenes, carbon nanotubes, and carbon quantum dots (QDs) (Fig. 1-3).

The work of Geim and Novoselov inaugurated enormous research efforts on graphene，which showed extraordinary characteristics of only a monolayer 0.34 nm thick graphene, such as outstanding durability and flaccidity, large lateral area, high thermal and electrical conductivity, extraordinary room-temperature mobility, electrical carrier performance of Dirac massless Fermions, an atypical quantum Hall effect at room temperature, and others.[3,8,9] Graphene has excited not only among science but also motivated as a host of various possibility for applications including, including transistors,[10-12] sensors,[13,14] luminescent devices,[15-17] thermal interface materials,[18,19] and piezo elements.

However, efforts to employ graphene for specific utilization were challenged by a difference of practical obstacles.

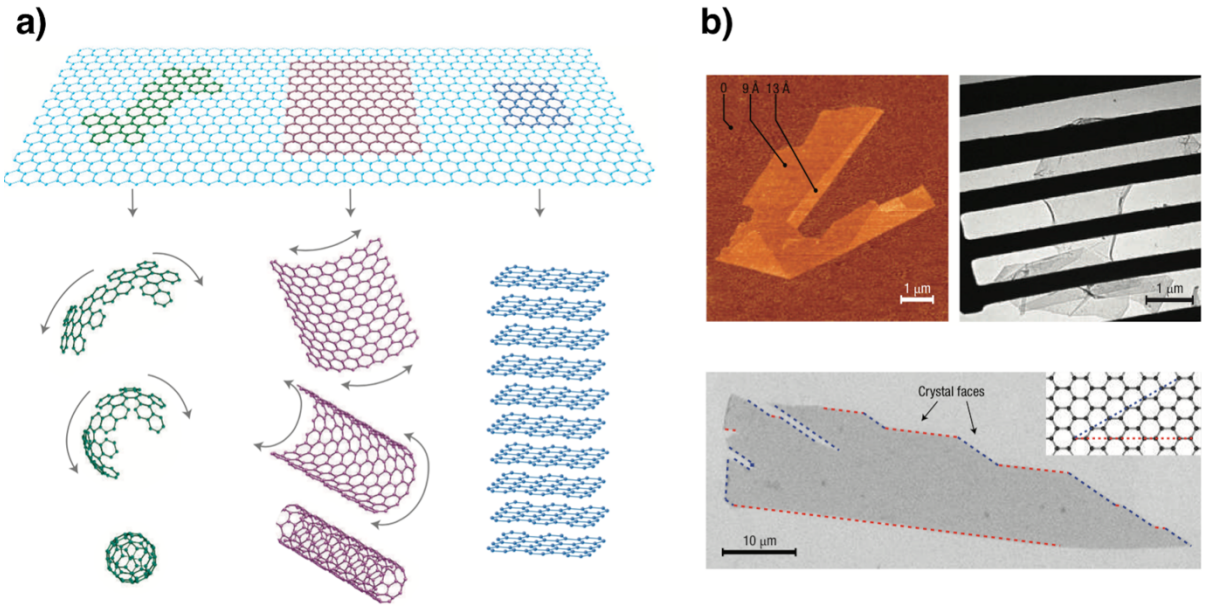

Fig. 1-3 | Graphene. **a)** Mother of all graphitic forms. Graphene is a 2D building material for carbon materials of all other dimensionalities. **b)** The microscopic images of one-atom-thick single crystals of graphene. Adapted by permission from Macmillan Publishers Ltd: Nature Chemistry ref. 3, copyright 2004.

For instance, the gapless essence of graphene, which causes the invention of semiconducting graphene-founded devices hard with lower switching current rates (I_{ON}/I_{OFF} < 100),[20] and a moderate performance in real circuit applications.[21,22] Graphene nanoribbons are semiconducting with the possibility of tuning out band gap, but their low electronic conductivities are incompetent for device fabrication.[8] Furthermore, doping of graphene by replacing C atoms with hetero-atoms is ungovernable and inadequate for nano-electronic applications.[23] Deficiencies of graphene in functional applications have prompted attempts of prolonging the graphene species to crystalline two-dimensional layered materials composed of other elements.[24] Substitution of C by N in graphene is a likely approach to the formation of graphene-like two-dimensional substances. Amorphous carbon nitride films with N/C ratios up to one-third were extensively studied in the past, but they are certainly not 2D crystalline layered materials. [25] Since 2009, graphitic C_3N_4, a kind of crystalline material that can be exfoliated to form film-like structure, is extensively studied. This kind of material is porous and contains holes due to a widely presenting of N atoms. Graphitic C_3N_4 is another semiconductive graphene-like material with a bandgap of

2.76 eV and attractive photocatalytic features.[26,27] Moreover, an ordered carbon nitride material with high crystallinity termed C_2N-h2D was published recently.[28] C_2N- h2D, contains uniform pores in its crystalline structure, is a semiconducting material with a bandgap of 1.96 eV, making it likely a better photo-catalyst for solar water splitting than C_3N_4. A field-effect transistor (FET) made of C_2N-h2D shows an on/off ratio (I_{ON}/I_{OFF} ratio) over 100. The theoretical calculation has examined the composition and endurance of regulated carbon nitride planar structures with different C/N ratios.[24]

Finally, C_3N consists of a 2D honeycomb structure with a homogeneous distribution of nitrogen atoms were reported. It appeared an even small bandgap of 0.39 eV. FET made of single-layer C_3N display an on–off current ratio surprisingly reached 5.5×10^{10} (Fig. 1-4).[29]

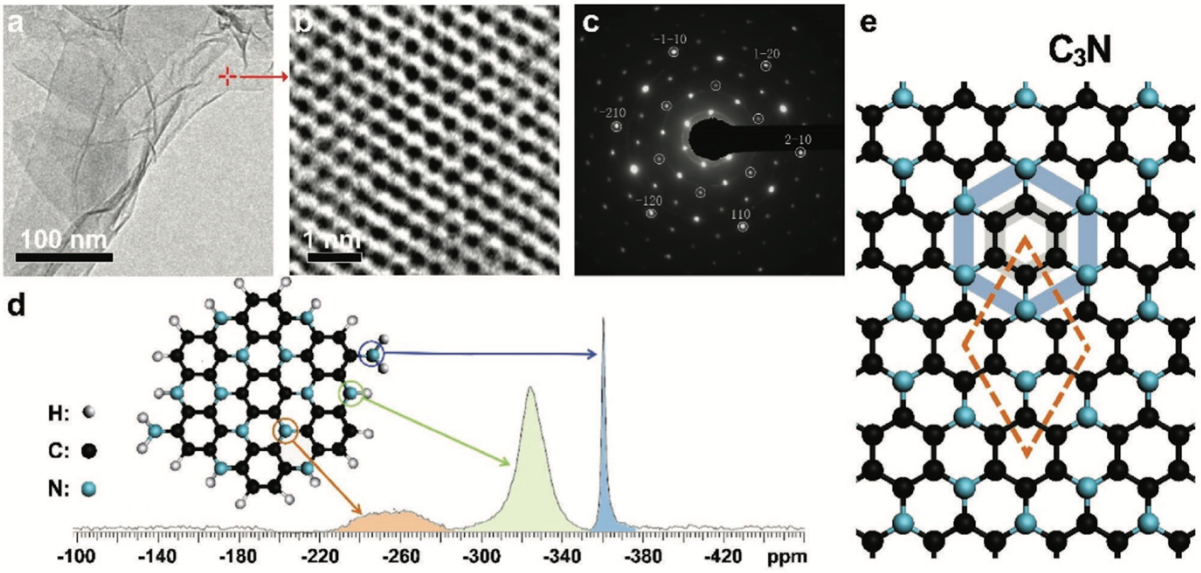

Fig. 1-4 | Structure of C_3N sheets. **a)** TEM image of a mixture of single- and multilayer C_3N sheets. **b)** HRTEM image showing the honeycomb structure. **c)** SAED indicating the D_{6h}-symmetry of N and C atoms in the single-layer C_3N sheet. **d)** ^{15}N-NMR spectrum of a mixture of single-layer and multilayer C_3N sheets. **e)** The molecular structure of the C_3N crystal. Adapted from ref. 29. Copyright 2017 by John Wiley & Sons, Inc.

1-2-3 Inorganic nanosheets

Knowing the importance of metal components, and further encouraged by unique properties of the two-dimensional material, scientists are stimulated to study other types of nanosheet: inorganic nanosheet. Single atomic layers of boron nitride, metal dichalcogenides, metal oxides and metal hydroxides *et al.* are called inorganic nanosheets. The research among these topics typically focused on nanosheets fabricated by top-down methods. Inorganic substances with a layered structure, such as BN, MoS_2, WS_2, $MoSe_2$, $MoTe_2$, $TaSe_2$, $NbSe_2$, $NiTe_2$, Bi_2Te_3,[7,30-33] perovskite oxide,[34] are possible materials which can strip down to their monolayers (*vide infra*) (Fig. 1-5). These materials have been investigated not only their primary electronic or magnetic characteristics but also employment for devices of energy generation or storage applications.[35,36]

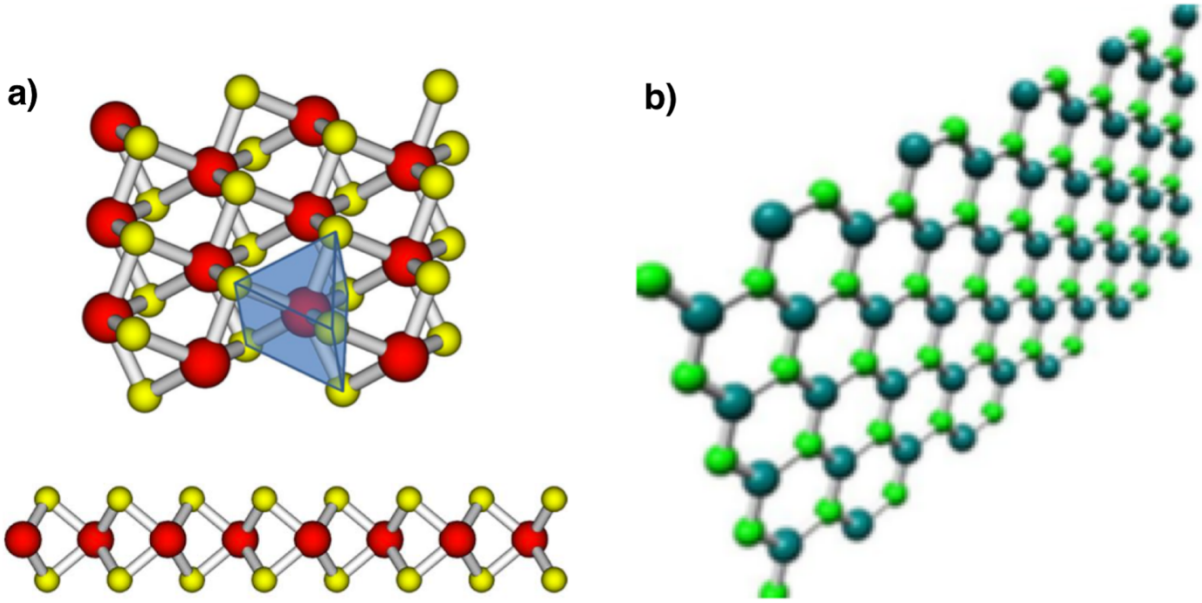

Fig. 1-5 | Structure of inorganic nanosheet. **a)** Structure of molybdenum disulfide, MoS_2. Yellow and red spheres represent sulfur atoms and molybdenum atoms respectively. b) Structure of boron nitride, BN. Dark green and light green spheres represent boron atoms and nitrogen atoms respectively.

1-3 Fabrication approaches of low-dimensional nanomaterials

1-3-1 Top-down method

As mentioned in the previous section (section 1-2-2), some inorganic bulk crystals occupy lamella arrangements, which suggests that they can exfoliate to two-dimensional materials. Geim group got a single layer of graphene by repeated peeling of highly oriented pyrolytic graphite and washed off by organic solvents such as acetone and ethanol; this monolayer sheet can be transferred to the various substrate by the scoop-up method. Such approach is called as mechanical exfoliation (Fig. 1-6).[3] This method was first applied to the preparation of crystals such as BN and TMD. The resulting two-dimensional material is stable under ambient conditions and exhibits a macro continuous high crystallinity. Mechanical exfoliation is the easiest and fastest way to synthesise a single-layered two-dimensional material, which only relies on shear forces during the peeling process without the use of other chemical reagents; thus, the complete structure of the raw material crystals is preserved. However, this preparation method is often obtained by a multi-layer, the single-layer ratio is very miniature so that this method is only applicable to small-scale laboratory preparation and cannot play a role in practical industrial engineering applications.

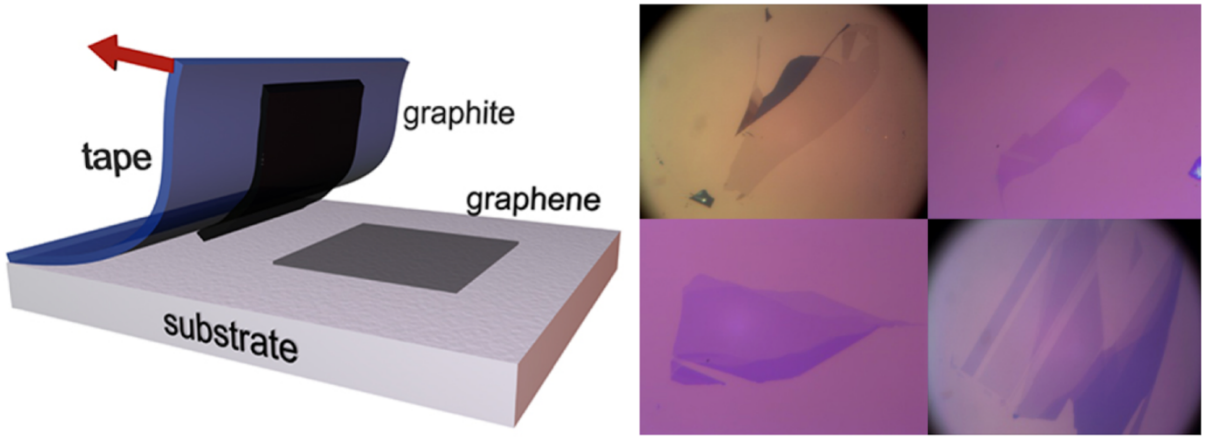

Fig. 1-6 | Schematic representation of the mechanical exfoliation. Process and microscope images of graphene flakes (single-, bi- and tri-layer samples).[3]

Liquid-phase exfoliation method is another important method for the preparation of nano-layers, including oxidation, doping, ion exchange, ultrasonic separation, electrochemical methods.[37] Oxidation is mainly used in the preparation of graphene, such as graphite flakes treated

with sulfuric acid, nitric acid or sulfuric/ nitric mixed acid, and then by adding potassium chlorate, potassium permanganate and other oxidants treatment, which makes the graphite oxidized and produced a large number of oxygen-containing functional groups. Followed by dispersion in polar solvents or with ultrasonic.

The ion doping method increases the interlayer spacing and reduces the interlaminar force by doping or exchanging the intergranular species, thus achieving the purpose of separating the layers and layers. For example, TiO_2-layered crystals tend to exhibit negative charge, and charge can be balanced by caesium ions. Therefore, for the negatively charged oxide, the purpose of separation can be achieved by using a mass ion exchange method such as tetrabutylammonium ion (Fig. 1-7).[38] Quantitative ion-inserted layered compounds can also be prepared by electrochemical methods.[39]

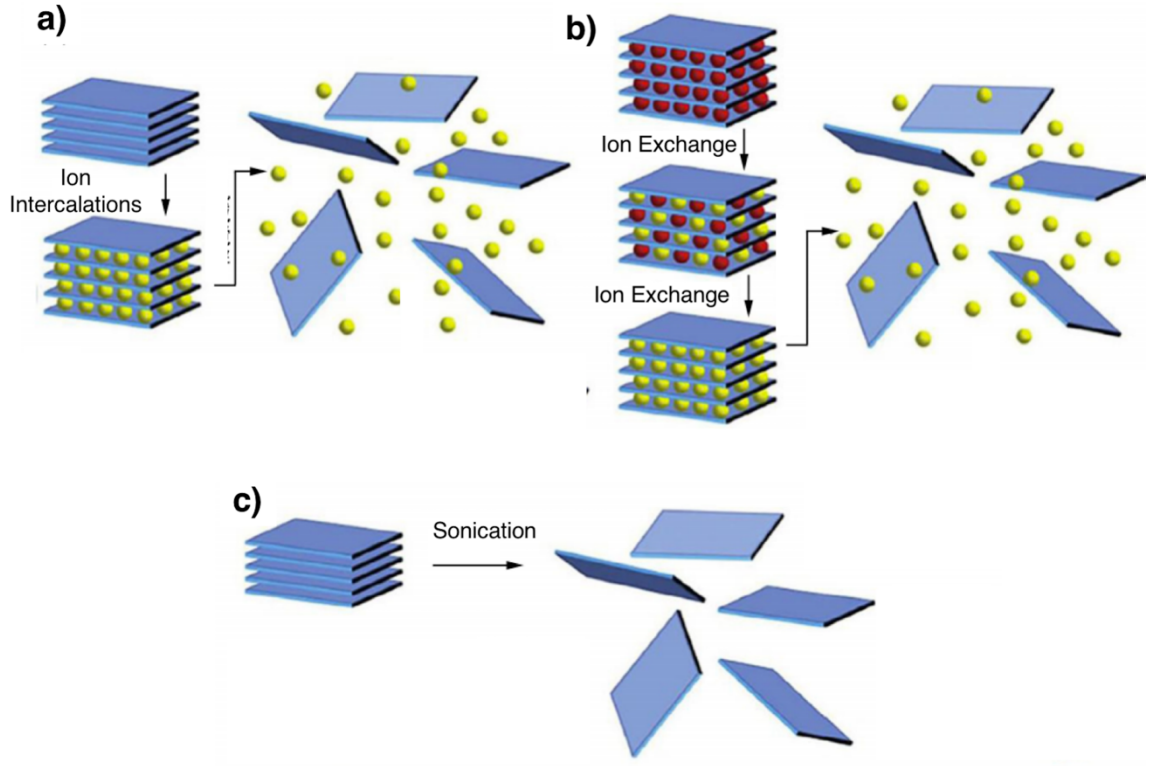

Fig. 1-7 | Schematic representation of the liquid-phase exfoliation. **a)** Ion intercalations exfoliation. **b)** Ion exchange exfoliation. **c)** Sonication exfoliation.

1-3-2 Bottom-up method

Because of top-down nanosheets lack tunability and variation limitation, bottom-up nanosheets show more potential among different application. This series of nanosheets is designed and fabricated directly from atomic, ionic and molecular components, namely classified as bottom-up nanosheets. The notion itself originated nearly a century ago, yet synthesis strategies and characterization methods objectified recently.[40]

The chemical vapour deposition (CVD) method is to vaporize the reactants and deposit the product on the substrate (Fig. 1-8). The biggest advantage of this method is the ability to produce relatively pure monolayer or oligomeric materials without the presence of thicker by-products. The matrix template can also be used as a catalyst for the growth of solid films, such as polycrystalline nickel foils and copper foils for the growth of BN nano-sized thin layers is an excellent catalytic substrate.[41] Table 1 shows the CVD conditions under various conditions that have been developed. According to the furnace, pressure can be divided into atmospheric pressure (APCVD), low pressure (LPCVD), high vacuum (UHVCVD). According to the gasification method can be divided into simple pyrolysis (Thermal CVD) and plasma (PECVD), which can be by the glow discharge or microwave (MPCVD), *etc.*

The method of preparing crystals from liquid phase under high temperature and high vapour pressure is called hydrothermal syntheses, such as MoS_2 or $MoSe_2$, such as ammonium heptamolybdate and sulphur or selenium in hydrazine hydrate solution.[42] Also, a monolayer material can be obtained by adding a surfactant. The method is easy to large-scale preparation, there is a certain application potential in industrial production.

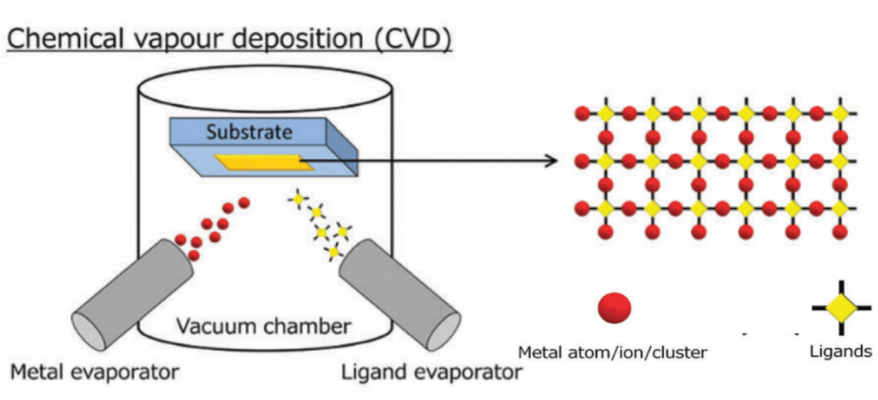

Fig. 1-8 | Schematic representation of CVD.

1-4 Coordination nanosheet

1-4-1 Introduction of coordination nanosheet

Another type of intriguing 2D material is coordination nanosheets (CONASHs),[43,44] which consist of metal complexes and can exhibit various unique physical and chemical features. They are easy to make by convenient bottom-up syntheses, because many coordination reactions proceed in solution under ambient conditions (Fig. 1-9). Initially, the characterization and structural analysis of CONASHs were the main focuses of research.[45-58] Recently, various functionalities of CONASHs have been demonstrated.[59-64]

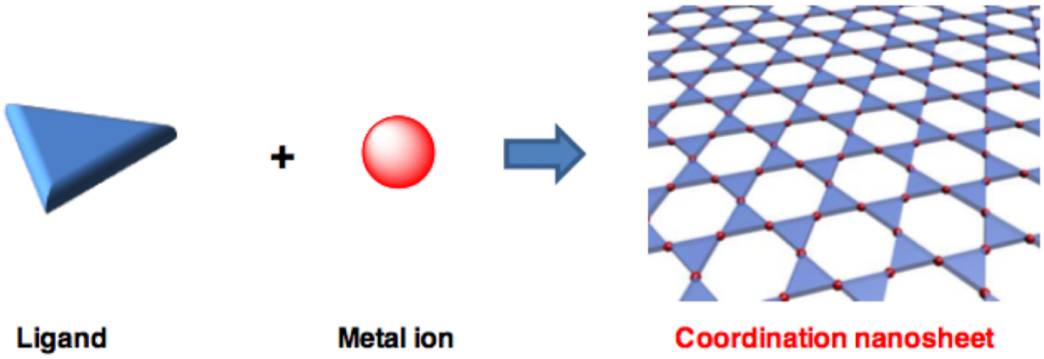

Fig. 1-9 | Schematic representation of CONASH. Adapted from ref. 48. Copyright 2014 American Chemical Society.

2D materials based on the bis(dithiolato)metal complex motif and its analogues constitute a significant group in CONASHs. Their square-planar geometry is exemplary for assembling 2D structures. Our first article [65] has incited their variations, in combination with metal ions with aromatic organic ligands, such as triphenylenehexaol,[66,67] benzenehexathiol,[65,68-70] triphenylenehexaamine,[67,71-74] triphenylenhexathiol,[75,76] and benzenehexaamine (Fig. 1-10).[77] The notable characteristics of this CONASH result from its electronic composition. The bis(dithiolene)metal(II) complex features quasi-aromatic property, which gives it a diversity of functionalities.[78,79] Moreover, multinuclear metalladithiolenes with units all tied to each other through mixed arene links experience electronic communication.[80-82]

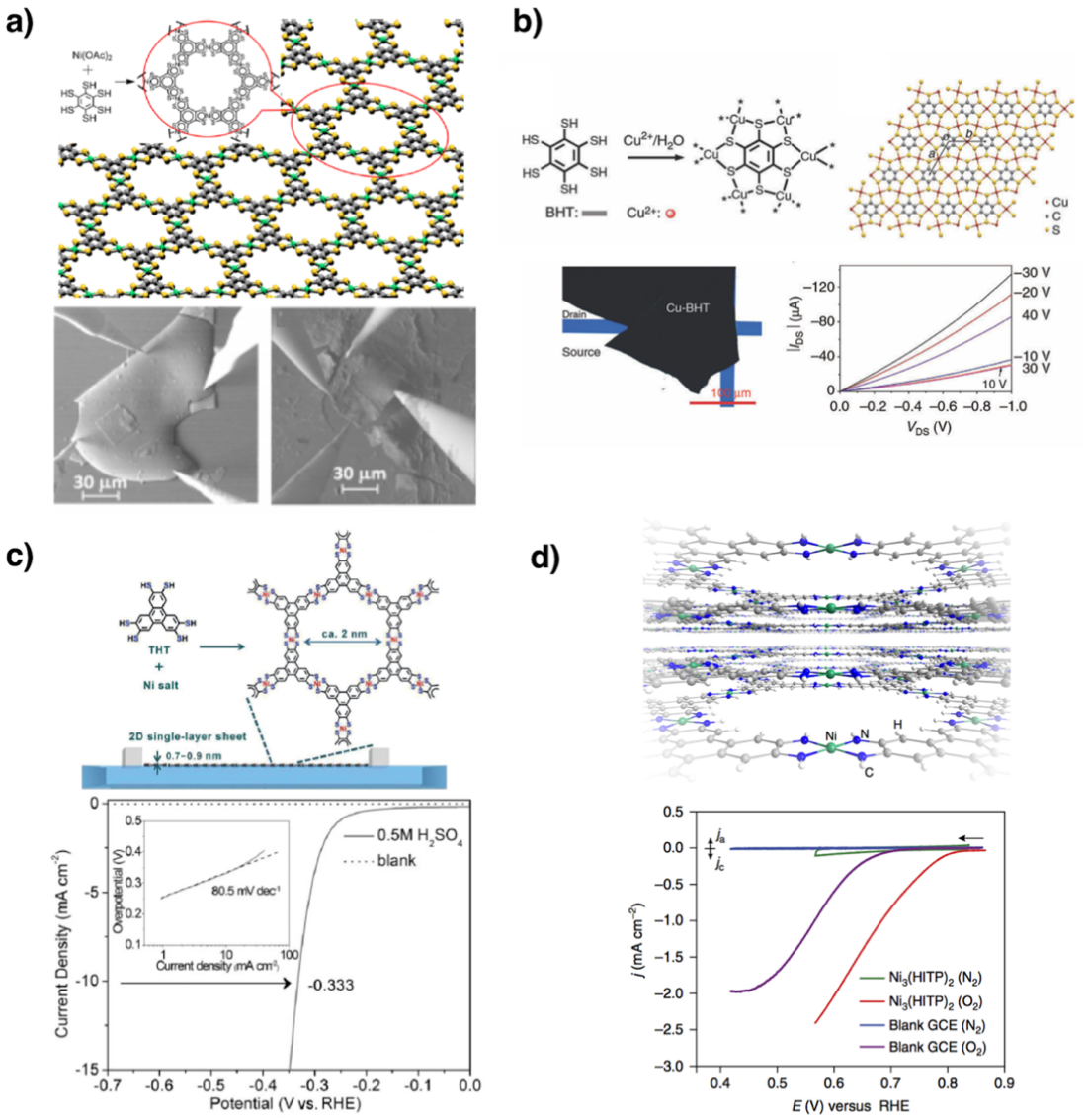

Fig. 1-10 | Example of CONASH. **a)** Illustration of the chemical structure of the nickel bis(dithiolene) complex nanosheet. **b)** Chemical composition and structure of Cu-BHT. And photograph of a bottom-gate bottom-contact FET based on Cu-BHT. **c)** Single-layer THTNi nanosheet generated at an air/water interface. And HER polarization plots for THTNi and a blank glassy carbon disk electrode in 0.5 M H_2SO_4. Structure of the $Ni_3(HITP)_2$ nanosheet (perspective view). **d)** ORR performance. Polarization curves for $Ni_3(HITP)_2$ under N_2 (green) versus O_2 atmosphere (red) Copyright 2014 American Chemical Society, 2015 Macmillan Publishers Limited, 2015 WILEY-VCH Verlag GmbH & Co. KGaA and 2015 Macmillan Publishers Limited.

Thus, it paves the π-conjugation over the 2D nanosheet. Some of these nanosheets show high electrical conductivity because of possessing strong charge delocalization in the extension,[59-74,83] even some of them been theoretically predicted to be 2D topological insulators.[84] Besides, these CONASHs can also perform as electrocatalysts: for instance, the hydrogen evolution reaction (HER) was catalysed by the bis(dithiolato)metal type of CONASHs.[75,85,86]

As explained in previous sections, tremendous attempts have been made to design two-dimensional nanomaterials. However, the homogeneous solution synthetic strategy is not able to control a random encounter between building blocks which generate undesired products. This problem strongly limits the convenient structural motifs. Under these circumstances, the method of a liquid/liquid or gas/liquid interface is an important strategy for developing the range of manufactured low-dimensional nanomaterials.

1-4-2 Liquid/liquid interface synthesis

Liquid/liquid interface synthesis has a long history of practice in polymer chemistry. In 1959, Wittbecker and Morgan manufactured nylon-6,10 by poly-condensation of sebacoyl chloride and hexamethylenediamine at an organic/aqueous interface.[87] Since the diacid chloride and diamine are dissolved in different immiscible solutions, the condensation reaction occurs only at the plane interface, whereby forming a thin sheet as a result. This method is called as interfacial polymerization and has been extensively used to fabricate various of polymers. In recent years, chemists have further expanded the utilization of the liquid/liquid interface to the fabrication of two-dimensional nanomaterials.

Liquid/liquid interfacial synthesis is valuable to produce multi-layered CONASHs (Fig. 2a). Typically, it requires gently overlaying an aqueous solution of one component on the top of an organic solution containing another component to form a liquid/liquid interface (Fig. 1-11). If the organic solvent has less density, than the layer arrangement change to the other way around. The coordination reaction at the liquid/liquid interface frequently fabricates multi-layer nanosheets; yet, fewer-layer nanosheet may also be formulated with adjustments in the system.

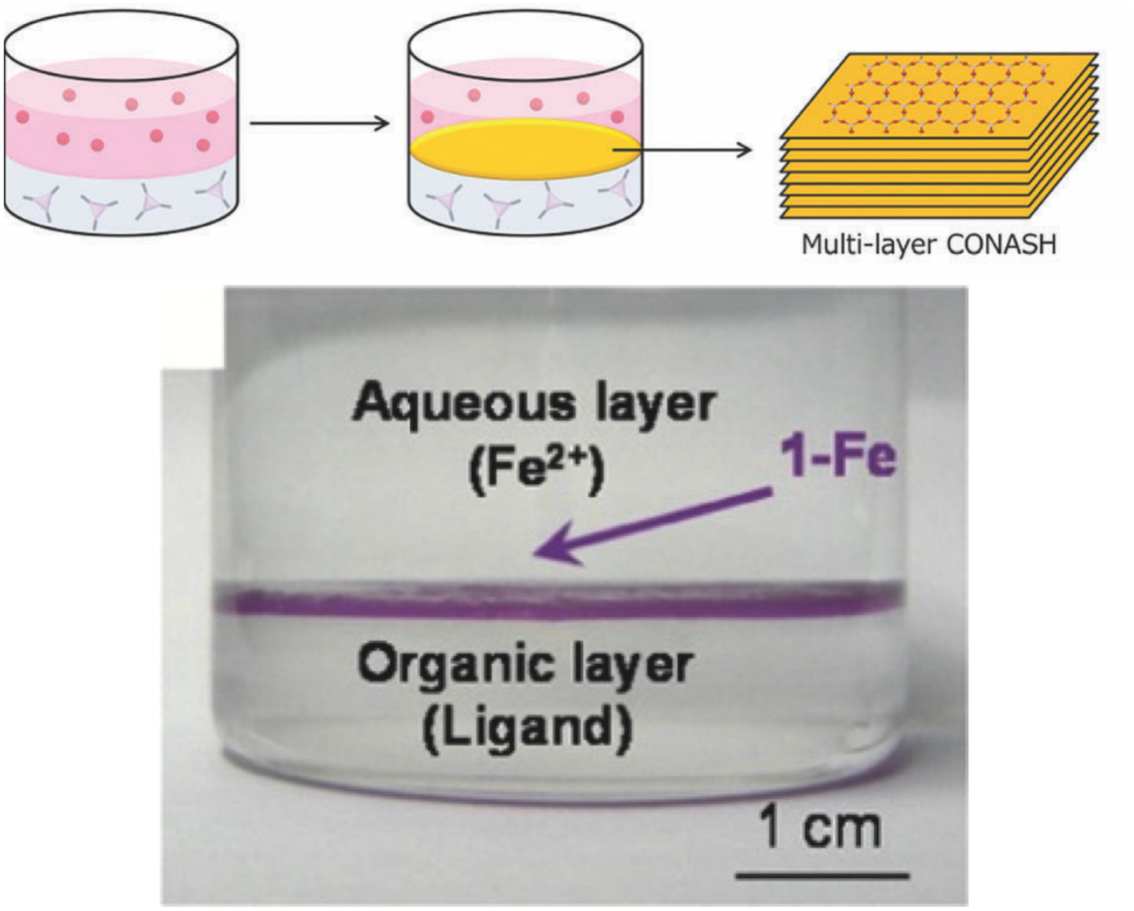

Fig. 1-11 | Bottom-up construction of LD nanomaterials at a liquid/liquid interface. Photograph of the liquid/liquid interfacial synthesis of bis(terpyridine)iron(II) complex nanosheet. Copyright 2015 American Chemical Society.[60]

1-4-3 Gas/liquid interface synthesis

More than a century ago, Langmuir observed that stearic acid spreads on a water facade (i.e. gas/water interface) with its carboxyl group in association with the water to form a molecularly thin 2D construction.[88] Since the hydrocarbon chain of each stearic acid molecule is approximately perpendicular to the water surface, the obtained film stresses uniform thickness and constitutional periodicity. His discovery has encouraged chemists to employ the gas/liquid interface as an approach of molecular structure. Gas/liquid interfacial synthesis is fitting for manufacturing few- or single-layer CONASHs (Fig. 12a). A small amount one component in an organic solvent is gently spread on an aqueous solution of the other ingredient. The prompt evaporation of the organic

solvent omits the ligand on the aqueous surface, and the coordination reaction proceeds at the gas/liquid interface. Conducting the synthesis in a Langmuir– Blodgett (LB) trough can conveniently fabricate tightly packed few- or single-layer CONASHs (Fig. 12b). The channel is loaded with an aqueous solution. Then, a diminutive quantity of component dissolved in organic solvent is scattered on the water surface. The evaporation of the organic solvent leads to pieces of a CONASH growing on the top of the water. The resultants can be collected by decreasing the surface area of the LB channel, which increases their density per unit area.

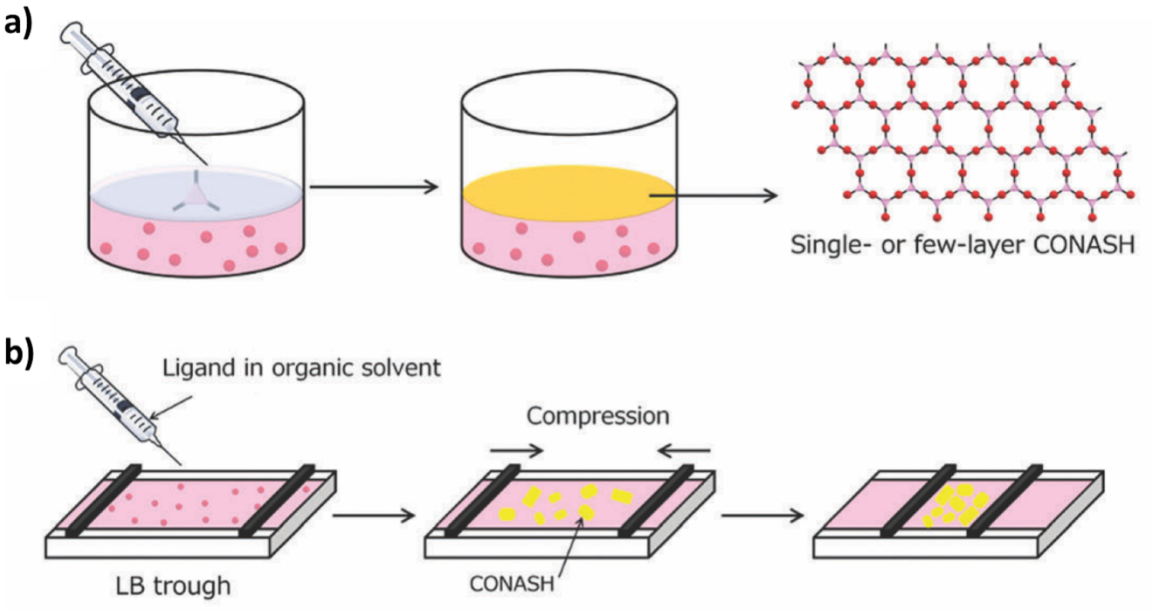

Fig. 1-12 | Schematic representation of gas/liquid interfacial synthesis. **a)** gas/liquid synthesis of single- or few-layer nanosheet. **b)** LB method.

1-5 Aim of the research in the Ph.D. course

Although CONASHs has been developed exhaustively due to its high potentials, yet fully adaption of coordination motifs to 2D architected material remains a serious challenge. Coordination nanosheets' variety has been limited by the high symmetric requirement of bridging ligands.

The aim of my Ph. D. research is to expand the field of CONASH by varying the bridging ligands with mixed ligating groups. By successively adapt motif with mixed ligating group into 2D material, we demonstrate coordination nanosheet can be precisely micro designed. Moreover, this work shows feasibility to let CONAH adapting less symmetric coordination motif which potentially can lead to design for targeted application.

As the first, I designed a π–conjugated CONASH comprising bis(iminothiolato)nickel moieties, NiIT, was synthesised by a reaction of $Ni(acac)_2$ with 1,3,5-triaminobenzene-2,4,6-trithiol (**L1**) in the presence of ferrocenium ion. I confirmed moiety adaptability by homogeneous synthesis and promoted to achieve two-dimensional nanoscale film-like material by liquid/liquid interfacial synthesis. Then I realized a crystalline π–conjugated bis(aminothiolato)nickel (**NiAT**) nanosheet could be synthesized by altering the liquid–liquid interfacial synthesis conditions of **NiIT**. Diffraction techniques confirmed the lateral and packing structure. Moreover, by gas-liquid interfacial synthesis, a single layered nanosheet was achieved. I investigated both **NiIT** and **NiAT** chemical compositions and physical properties by several measurements. Focusing on the redox activity, which achieved the switching functionality of conducting properties. Another class of CONASH with mixed ligating group comprise bis(iminophenolato)nickel (**NiIP**) moiety was also fabricated by different interfacial synthesis strategies, which showed impressive crystallinity. These studies demonstrate that CONASH can be precisely designed and tuned through fabrication synergies and chemical treatments, and a slight change of composition can dramatically change a nanosheet's properties. **NiIT** and **NiAT** are also subject for energy generation application studies, such as electrocatalyst for hydrogen evolution reaction.

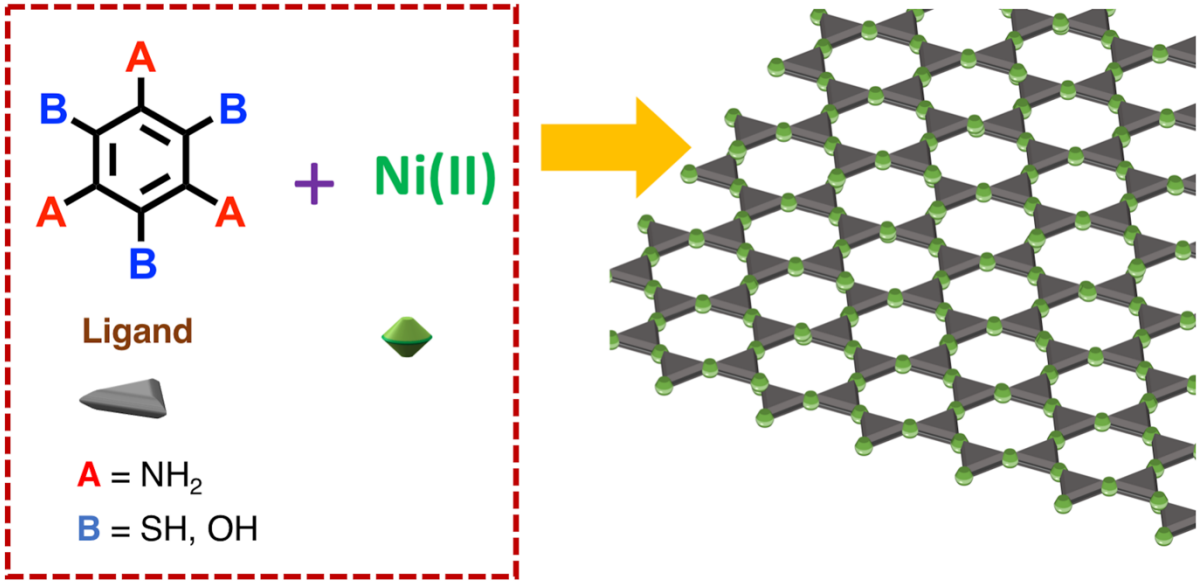

Fig. 1-13 | Conceptual scheme showing the studies in my Ph.D. course.

1-6 References

1 J. Liu, Y. Liu, N. Liu, Y. Han, X. Zhang, H. Huang, Y. Lifshitz, S. T. Lee, J. Zhong and Z. H. Kang, *Science,* 2015, **347**, 970.

2 W. A. Heer, A. Châtelain and D. Ugarte, *Science,* 1995, **270**, 1179.

3 K. S. Novoselov, *Science,* 2004, **306**, 666.

4 H. W. Kroto, J. R. Heath, S. C. O'Brien, R. F. Curl and R. E. Smalley, *Nature,* 1985, **318**, 162.

5 Y. Ohki, Y. Sunada, M. Honda, M. Katada and K. Tatsumi, *J. Am. Chem. Soc.,* 2003, **125**, 4052.

6 H. Maeda, R. Sakamoto, Y. Nishimori, J. Sendo, F. Toshimitsu, Y. Yamanoi and H. Nishihara, *Chem. Commun.*, 2011, **47**, 8644.

7 J. N. Coleman, M. Lotya, A. O'Neill, S. D. Bergin, P. J. King, U. Khan, K. Young, A. Gaucher, S. De, R. J. Smith, I. V. Shvets, S. K. Arora, G. Stanton, H.-Y. Kim, K. Lee, G. T. Kim, G. S. Duesberg, T. Hallam, J. J. Boland, J. J. Wang, J. F. Donegan, J. C. Grunlan, G. Moriarty, A. Shmeliov, R. J. Nicholls, J. M. Perkins, E. M. Grieveson, K. Theuwissen, D. W. McComb, P. D. Nellist and V. Nicolosi, *Science* 2011, **331**, 568.

8 A. K. Geim, K. S. Novoselov *Nat. Mater.* 2007, **6**, 183.

9 T.R. Wu, X. F. Zhang, Q. H. Yuan, J. C. Xue, G. Y. Lu, Z. H. Liu, H. S. Wang, H. M. Wang, F. Ding, Q. K. Yu, X. M. Xie and M. H. Jiang, *Nat. Mater.*, 2016, **15**, 43.

10 Q. H. Wang, K. Kalantar-Zadeh, A. Kis, J. N. Coleman and M. S. Strano, *Nat. Nanotechnol*., 2012, **7**, 699.

11 R. Cheng, S. Jiang, Y. Chen, Y. Liu, N. Weiss, H.-C. Cheng, H. Wu, Y. Huang and X. Duan, *Nat. Commun.,* 2014, **5**, 5143.

12 M. C. Lemme, T. J. Echtermeyer, M. Baus and H. Kurz, *IEEE Electron Device Lett.,* 2007, **28**, 282.

13 F. Schedin, A. K. Geim, S. V. Morzov, E. W. Hill, P. Blake, M. I. Katsnelson and K. S. Novoselov, *Nat. Mater.,* 2007, **6**, 652.

14 J. Yan, M.-H. Kim, J. A. Elie, A. B. Sushkov, G. S. Jenkins, H. M. Milchberg, M. S. Fuhrer and H. D. Drew, *Nat. Nanotechnol*., 2012, **7**, 472.

15 Y. D. Kim, H. Kim, Y. Cho, J. H. Ryoo, C.-H. Park, P. Kim, Y. S. Kim, S. Lee, Y. Li, S.-N. Park, Y. S. Yoo, D. Yoon, V. E. Dorgan, E. Pop, T. F. Heinz, J. Hone, S.-H. Chun, H. Cheong, S. W. Lee, M.-H. Bae and Y. D. Park, *Nat. Nanotechnol*., 2015, **10**, 676.

16 Y. J. Zhang, T. Oka, R. Suzuki, J. T. Ye and Y. Iwasa, *Science,* 2014, **344**, 725.

17 S. Mouri, Y. Miyauchi and K. Matsuda, *Nano Lett.,* 2013, **13**, 5944.

18 Q. Liang, X. Yao, W. Wang, Y. Liu and C. P. Wong, *ACS Nano,* 2011, **5**, 2392.

19 K. M. F. Shahil and A. A. Balandin, *Nano Lett.,* 2012, **12**, 861.

20 K. Kim, J. Y. Choi, T. Kim, S. H. Cho, H. J. Chung, *Nature*, 2011, **479**, 338.

21 F. Schwierz, *Nat. Nanotechnol.,* 2010, **5**, 487.

22 I. Meric, M. Y. Han, A. F. Young, B. Ozyilmaz, P. Kim, K. L. Shepard, *Nat. Nanotechnol.,* 2008, **3**, 654.

23 A. C. Ferrari, F. Bonaccorso, V. Fal'ko, K. S. Novoselov, S. Roche, P. Bøggild, S. Borini, F. H. L. Koppens, V. Palermo, N. P. Klm, J. A. Garrido, R. Sordan, A. Bianco, L. Ballerini, M. Prato, E. Lidorikis, J. Kivioja, C. Marinelli, T. Ryhänen, A. Morpurgo, J. N. Coleman, V. Nicolosi, L. Colombo, A. Fert, M. Garcia-Hernandez, A. Bachtold, G. F. Schneider, F. Guinea, C. Dekker, M. Barbone, Z. P. Sun, C. Galiotis, A. N. Grigorenko, G. Konstantatos, A. Kis, M. Katsnelson, L. Vandersypen, A. Loiseau, V. Morandi, D. Neumaier, E. Treossi, V. Pellegrini, M. Polini, A. Tredicucci, G. M. Williams, B. H. Hong, J. H. Ahn, J. M. Kim, H. Zirath, B. J. Wees, H. Zant, L. Occhipinti, A. D. Matteo, I. A. Kinloch, T. Seyller, E. Quesnel, X. L. Feng, K. Teo, N. Rupesinghe, P. Hakonen, S. R. T. Neil, Q. Tannock, T. Löfwander, J. Kinaret, *Nanoscale,* 2015, **7**, 4598.

24 Y. Feng, X. Yao, M. Wang, Z. Hu, X. Luo, H. T. Wang, L. Zhang, *J Chem. Phys.*, 2013, **138**, 164706.

25 S. Muhl, J. M. Mendez, *Diamond Relat. Mater.*, 1999, **8**, 1809.

26 X. Wang, K. Maeda, A. Thomas, K. Takanabe, G. Xin, J. M. Carlsson, K. Domen, M. Antonietti, *Nat. Mater.*, 2009, **8**, 76.

27 J. Liu, Y. Liu, N. Liu, Y. Han, X. Zhang, H. Huang, Y. Lifshitz, S. T. Lee, J. Zhong, Z. H. Kang, *Science*, 2015, **347**, 970.

28 J. Mahmood, E. K. Lee, M. Jung, D. B. Shin, I. Y. Jeon, S. M. Jung, H. J. Choi, J. M. Seo, S. Y. Bae, S. D. Sohn, N. Park, J. H. Oh, H. J. Shin, J. B. Baek, *Nat. Commun.*, 2015, **6**, 6486.

29 S. Yang, W. Li, C. Ye, G. Wang, H. Tian, C. Zhu, P. He, G. Q. Ding, X. M. Xie, Y. Liu, Y. Lifshitz, S.-T. Lee, Z. H. Kang, M. H. Jiang, *Adv. Mater.*, 2017, **29**, 1605625.

30 J. –O. Joswig, T. Lorenz, T. B. Wendumu, S. Gemming, G. Seifert, *Acc. Chem. Res.*, 2014, **48**, 48.

31 C. R. Dean, A. F. Young, I. Meric, C. Lee, L. Wang, S. Sorgenfrei, K. Watanabe, T. Taniguchi, P. Kim, K. L. Shepard, J. Hone, *Nat. Nanotech.,* 2010, **5**, 722.

32 K. S. Novoselov, D. Jiang, F. Schedin, T. J. Booth, V. V. Khotkevich, S. V. Morozov, A. K. Geim, *PNAS*, 2005, ***102***, 10451.

33 B. Radisavljevic, A. Radenovic, J. Brivio, V. Giacometti, A. Kis, *Nat. Nanotech.*, **2011**, *6*, 147.

34 B. -W. Li, M. Osada, T. C. Ozawa, Y. Ebina, K. Akatsuka, R. Ma, H. Funakubo, T. Sasaki, *ACS Nano*, 2010, **4**, 6673.

35 T. F. Jaramillo, K. P. Jørgensen, J. Bonde, J. H. Nielsen, S. Horch, I. Chorkendorff, *Science*, 2007, **317**, 100.

36 Z. W. She, J. Kibsgaard, C. F. Dickens, I. Chorkendorff, J. K. Nørskov and T. F. Jaramillo, *Science*, 2017, **355**, 155.

37 V. Nicolosi, M. Chhowalla, M. G. Kanatzidis, M. S. Strano, J. N. Coleman, *Science*, 2013, **340**, 1226419.

38 S. Ida, D. Shiga, M. Koinuma, Y. Matsumoto, *J. Am. Chem. Soc.*, 2008, **130**, 14038.

39 Z. Y.Zeng, Z. Y. Yin, X. Huang, H. Li, Q. Y. He, G. Lu, F. Boey, H. Zhang, *Angew. Chem. Int. Edit.*, 2011, **50**, 11093.

40 J. Sakamoto, J. van Heijst, O. Lukin, A. D. Schlüter, *Angew. Chem. Int. Ed.*, 2009, **48**, 1030.

41 Q. Tang, Z. Zhou, *Prog. Mater. Sci.* 2015, **58**, 1244.

42 Y. Y. Peng, Z. Y. Meng, C. Zhong, J. Lu, W. C. Yu, Y. B. Jia, Y. T. Qian, *Chem. Lett.*, 2001, **30**, 772.

43 M. T. Ong and E. J. Reed, *ACS Nano,* 2012, **6**, 1387.

44 W. Wu, L. Wang, Y. Li, F. Zhang, L. Lin, S. Niu, D. Chenet, X. Zhang, Y. Hao, T. F. Heinz, J. Hone and Z. L. Wang, *Nature,* 2014, **514**, 470.

45 A. Dmitriev, H. Spillmann, N. Lin, J. V. Barth and K. Kern, *Angew. Chem. Int. Ed.,* 2003, **42**, 2670.

46 W. Xu, J.-G. Wang, M. Yu, E. Laegsgaard, I. Stensgaard, T. R. Linderoth, B. Hammer, C. Wang and F. Besenbacher, *J.Am.Chem.Soc.,* 2010, **132**, 15927.

47 Y. Li, J. Xiao, T. E. Shubina, M. Chen, Z. Shi, M. Schmid, H.-P. Steinrück, M. Gottfried and N. Lin, *J. Am. Chem. Soc.,* 2012, **134**, 6401.

48 C. S. Kley, J. Čechal, T. Kumagai, F. Schramm, M. Ruben, S. Stepanow and K. Kern, *J. Am. Chem. Soc.,* 2012, **134**, 6072.

49 Z. Shi and N. Lin, *J. Am. Chem. Soc.,* 2009, **131**, 5376.

50 J. Liu, T. Lin, Z. Shi, F. Xia, L. Dong, P. N. Liu and N. Lin, *J. Am. Chem. Soc.,* 2011, **133**, 18760.

51 H. Walch, J. Dienstmaier, G. Eder, R. Gutzler, S. Schlögl, T. Sirtl, K. Das, M. Schmittel and M. Lackinger, *J. Am. Chem. Soc.,* 2011, **133**, 7909.

52 T.-C. Tseng, N. Abdurakhmanova, S. Stepanow and K. Kern, *J. Phys. Chem. C*., 2011, **115**, 10211.

53 Z. Shi and N. Lin, *J. Am. Chem. Soc.,* 2010, **132**, 10756.

54 M. Matena, M. Stöhr, T. Riehm, J. Björk, S. Martens, M. S. Dyer, M. Persson, J. Lobo-Checa, K. Müller, M. Enache, H. Wadepohl, J. Zegenhagen, T. A. Jung and L. H. Gade, *Chem. - Eur. J.,* 2010, **16**, 2079.

55 J. A. A. W. Elemans, S. Lei and S. D. Feyter, *Angew. Chem. Int. Ed*., 2009, **48**, 7298.

56 S. Motoyama, R. Makiura, O. Sakata and H. Kitagawa, *J. Am. Chem. Soc.,* 2011, **133**, 5640.

57 R. Makiura, S. Motoyama, Y. Umemura, H. Yamanaka, O. Sakata and H. Kitagawa, *Nat. Mater.*, 2010, **9**, 565.

58 S. Stepanow, N. Lin, D. Payer, U. Schlickum, F. Klappenberger, G. Zoppellaro, M. Ruben, H. Brune, J. V. Barth and K. Kern, *Angew. Chem. Int. Ed.,* 2007, **46**, 710.

59 T. Kambe, T. Kusamoto, R. Sakamoto and H. Nishihara, *Macromol. Symp.,* 2015, **351**, 78.

60 K. Takada, R. Sakamoto, S.-T. Yi, S. Katagiri, T. Kambe and H. Nishihara, *J. Am. Chem. Soc.,* 2015, **137**, 4681.

61 R. Sakamoto, K. Hoshiko, Q. Liu, T. Yagi, T. Nagayama, S. Kusaka, M. Tsuchiya, Y. Kitagawa, W.-Y. Wong and H. Nishihara, *Nat. Commun.,* 2015, **6**, 6713.

62 R. Sakamoto, T. Iwashima, M. Tsuchiya, R. Toyoda, R. Matsuoka, J. F. Kögel, S. Kusaka, K. Hoshiko, T. Yagi, T. Nagayama, H. Nishihara, *J. Mater. Chem. A,* 2015, **3**, 15357.

63 R. Sakamoto, K. Takada, X. Sun, T. Pal, T. Tsukamoto, E. J. H. Phua, A. Rapakousiou, K. Hoshiko and H. Nishihara, *Coord. Chem. Rev.,* 2016, **320-321**, 118.

64 H. Maeda, R. Sakamoto and H. Nishihara, *Langmuir,* 2016, **32**, 2527.

65 T. Kambe, R. Sakamoto, K. Hoshiko, K. Takada, M. Miyachi, J. H. Ryu, S. Sasaki, J. Kim, K. Nakazato, M. Takata and H. Nishihara, *J. Am. Chem. Soc.,* 2013, **135**, 2462.

66 M. Hmadeh, Z. Lu, Z. Liu, F. Gándara, H. Furukawa, S. Wan, V. Augustyn, R. Chang, L. Liao, F. Zhou, E. Perre, V. Ozolins, K. Suenaga, X. Duan, B. Dunn, Y. Yamamto, O. Terasaki and O. M. Yaghi, *Chem. Mater.,* 2012, **24**, 3511.

67 M. G. Campbell, S. F. Liu, T. M. Swager and M. Dincă, *J.Am.Chem.Soc.*, 2015, **137**, 13780.

68 K. Hoshiko, T. Kambe, R. Sakamoto, K. Takada and H. Nishihara, *Chem. Lett.,* 2014, **43**, 252.

69 T. Pal, T. Kambe, T. Kusamoto, M. L. Foo, R. Matsuoka, R. Sakamoto and H. Nishihara, *Chem- PlusChem,* 2015, **80**, 1255.

70 X. Huang, P. Sheng, Z. Tu, F. Zhang, J. Wang, H. Geng, Y. Zou, C.-a. Di, Y. Yi, Y. Sun, W. Xu and D. Zhu, *Nat. Commun.*, 2015, **6**, 7408.

71 D. Sheberla, L. Sun, M. Blood-Forsythe, S. Er, C. R. Wade, C. K Brozek, A. Aspuru-Guzik and M. Dincă, *J. Am. Chem. Soc.* 2014, **136**, 8859.

72 E. M. Miner, T. Fukushima, D. Sheberla, L. Sun, Y. Surendranath and M. Dinc˘a, *Nat. Commun.*, 2015, **7**, 10942.

73 D. Sheberla, J. C. Bachman, J. S. Elias, C.-J.Sun, Y.Shao-Hornand and M. Dincă, *Nat. Mater.*, 2016, **16**, 220.

74 M. G. Campbell, D. Sheberla, S. F. Liu, T. M. Swager and M. Dincă, *Angew. Chem. Int. Ed.*, 2015, **54**, 4349.

75 R. Dong, M. Pfeffermann, H. Liang, Z. Zheng, X. Zhu, J. Zhang and X. Feng, *Angew. Chem. Int. Ed.,* 2015, **54**, 12058.

76 J. Cui and Z. Xu, Chem. Commun., 2014, **50**, 3986.

77 N. Lahiri, N. Lotfizadeh, R. Tsuchikawa, V. Deshpande and J. Louie, *J. Am. Chem. Soc.,* 2017, **139**, 19.

78 P. Cassoux, Coord. Chem. Rev., 1999, **185–186**, 213.

79 R. Kato, *Chem. Rev.*, 2004, **104**, 5319.

80 I. Matsuoka, K. Aramaki and H. Nishihara, J. Chem. Soc., *Dalton Trans.*, 1998, 147

81 Y. Shibata, B. Zhu, S. Kume and H. Nishihara, *Dalton Trans.*, 2009, 1939

82 T. Kambe, S. Tsukada, R. Sakamoto and H. Nishihara, *Inorg. Chem.*, 2011, **50**, 6856.

83 T. Kambe, R. Sakamoto, T. Kusamoto, T. Pal, N. Fukui, K. Hoshiko, T Shimojima, Z. Wang, T. Hirahara, K. Ishizaka, S. Hasegawa, F. Liu and H. Nishihara, *J. Am. Chem. Soc.,* 2014, **136***,* 14357.

84 Z. F. Wang, N. Su and F. Liu, *Nano Lett.,* 2013, **13***,* 2842.

85 R. Dong, Z. Zheng, D. C. Tranca, J. Zhang, N. Chandrasekhar, S. Liu, X. Zhuang, G. Seifert and X. Feng, *Chem. - Eur. J.,* 2016, **23**, 2255.

86 A. J. Clough, J. W. Yoo, M. H. Mecklenburg and S. C Marinescu, *J. Am. Chem. Soc.,* 2015, **137**, 118.

87 Wittbecker, E. L.; Morgan, P. W. *J. Polym. Sci.*, 1959, **40**, 289.

88 I. Langmuir *J. Am. Chem. Soc.*, 1917, **39**, 1848–1906.

Chapter 2 π-Conjugated Bis(iminothiolato)nickel Nanosheet

2-1 Introduction

2-1-1 Multinuclear metal complexes

The investigation objective of recognizing synthetic approach to multinuclear metal complexes，which satisfy the needs for enhanced precise tuning of functionalities in the analogous mononuclear complexes continues to be an objection.[1] Multinuclear transition metal complexes with strong electronic communication have drawn much recognition from chemists. For example, the redox of multinuclear metal compound presents the change in magnetic and optical characteristics by adjusting their oxidation states, and hence they are the applicant of molecular switches and memories applicable to the molecular applications (Fig. 2-1).[1,2,3]

Trinuclear complexes with triangular shape have been investigated for a long time due to their unique characteristics such as mixed-valency[4-8] and spin frustrations.[9-15] These unique electronic and magnetic properties occur from the electronic communications among metals at the triangular position. Noticeably, the π–conjugated type particularly comprises interesting properties including the long-range transfer of electronic interactions and tuning of the properties by alterations of bridging ligands.

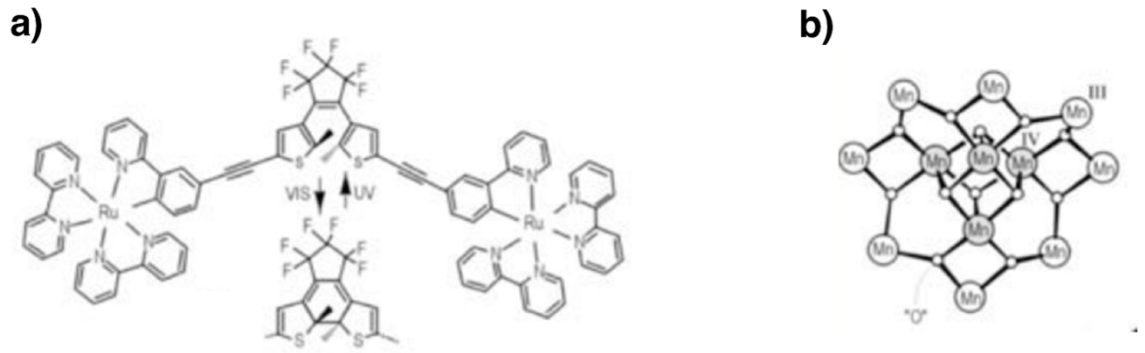

Fig. 2-1 | Example of multinuclear metal complexes. **a**) Wires; **b**) storage molecules that show promise for mono-molecular electronics. Adapted by permission from Macmillan Publishers Ltd: Nature ref. 1, copyright 2000.

2-1-1 Bis(iminothiolato) moiety

Compare with metalladithiolenes and metalladiimines, the descendant of the fusion of these two moieties, metallabisiminothiolenes, has rarely been studied. Despite the fact that aminothiophenolates ligand and its many organic derivatives have been broadly investigated; yet only a few crystal structures of complexes containing at least one aminothiolato moiety are available in the Cambridge Crystallographic Data Base. The redox activity of this type of ligand has rarely[16,17] been addressed in the past. Among most of those complexes, the aminothiophenolate part is believed to be redox innocent.[18] In 2001, Wieghardt and his respectful coauthors reported the redox performance of o-aminothiophenolates are noninnocent ligands (Fig. 2-2).[19] They showed that these diamagnetic neutral classes comprise a diamagnetic Ni^{II}, Pd^{II}, Pt^{II} (d8) central ion. The electronic formations of these complexes are best expressed as diradicals with a singlet ground state. The bis(iminothiolato) considering as an oxidized form which contain C-N and C-S bond display as double bond character from each single crystal structure. This motif is forming as square-planar and adopt a *trans*- configuration. Although, one may concern the formation could be cis, yet from previous study there are no report of Ni cis formed mononuclear crystal, the trans-formation will considerably as thermodynamically the favored form.

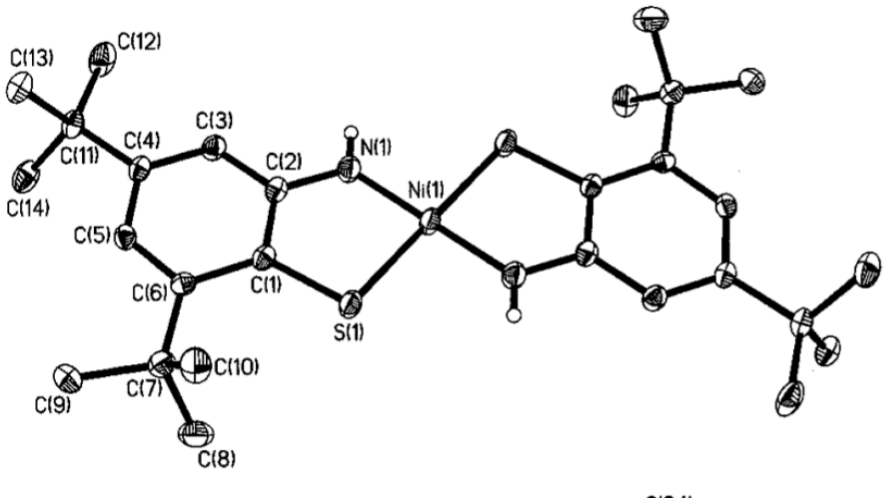

Figure 2-2 | Structure of the neutral molecules of Ni (2,4-di-tert-butyl-6-aminothiophenol)$_2$ complex.[19]

2-1-3 Aim of the present study

The intention of this study is to extend the field of CONASH by diversifying the bridging ligands with mixed functional groups (Fig. 2-3). Because of the redox and catalytic properties of S, NH-containing bis(1-iminobenzene-2-thiolato)nickel[19,20] are dissimilar to those of S-containing bis(benzene-1,2-dithiolato)nickel[21] and NH-containing bis(1,2-diiminobenzene)nickel,[22] so that unique properties of bis(iminothiolato)nickel (**NiIT**) nanosheet different from those of bis(dithiolato)nicke[23,24] and bis(diimino)nickel[25] nanosheets can be expected.

I synthesised **NiIT** sheets as a bulk material (**bulk-NiIT**) using a homogeneous reaction of Ni^{2+} with **L1** in the presence of an oxidising agent to verify the practicability of coordination moiety, and **NiIT** nanosheets (**nano-NiIT**) via liquid–liquid interfacial reaction. The interface can work as a 2D room for the reactants to accomplish well-defined sheet-like morphologies.

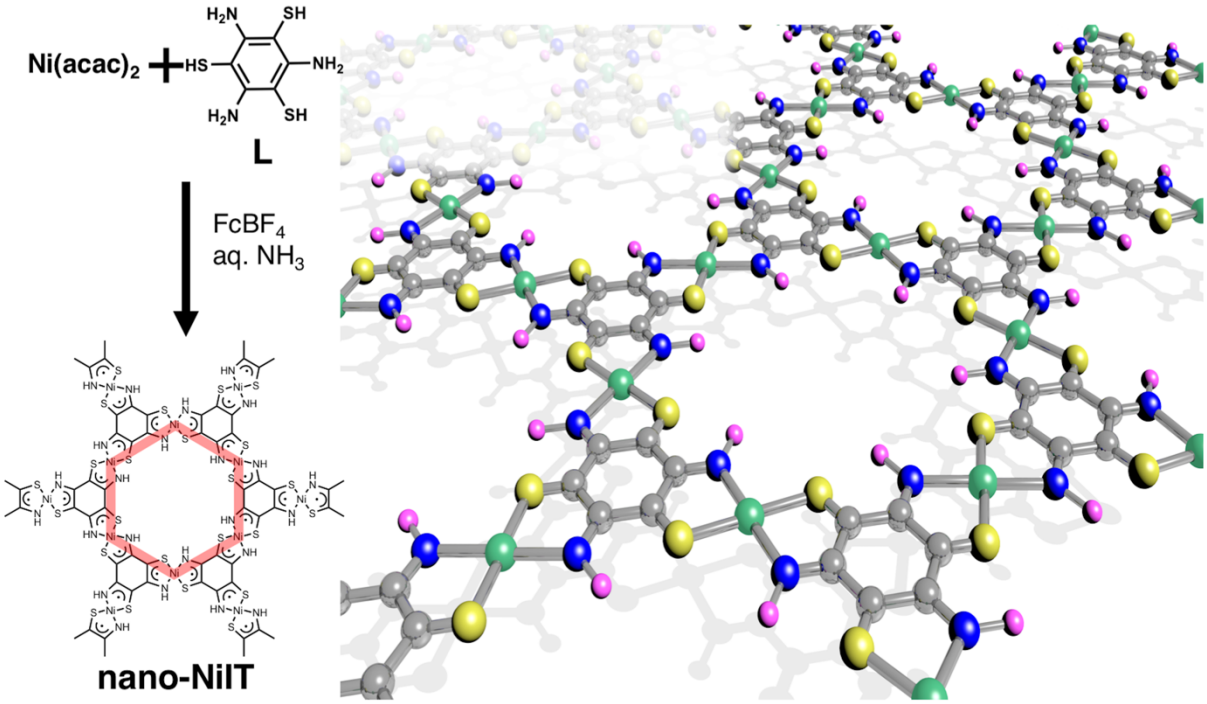

Fig. 2-3 | Schematic illustration of fabrication of bis(iminothiolato)nickel nanosheet, **nano-NiIT.** Grey, C; yellow, S; blue, N; purple H; green, Ni.

2-2 Experiment sections

2-2-1 Materials

All starting material and solvents were purchased from Tokyo Chemical Industry Co., Ltd. Dichloromethane was purified with a Glass Contour Solvent Dispensing System (Nikko Hansen & Co., Ltd.). Water was purified using the Milli-Q purification system (Merck). 1,3,5-Triaminobenzene-2,4,6-trithiol **(L1,** procedures are indicated in Fig. 2-4, overall yield 39.7%**)** and a mononuclear complex bis(1-aminobenzene-2-thiolato)nickel(II) [**NiIT-M**] were prepared according to the literature.[26,27]

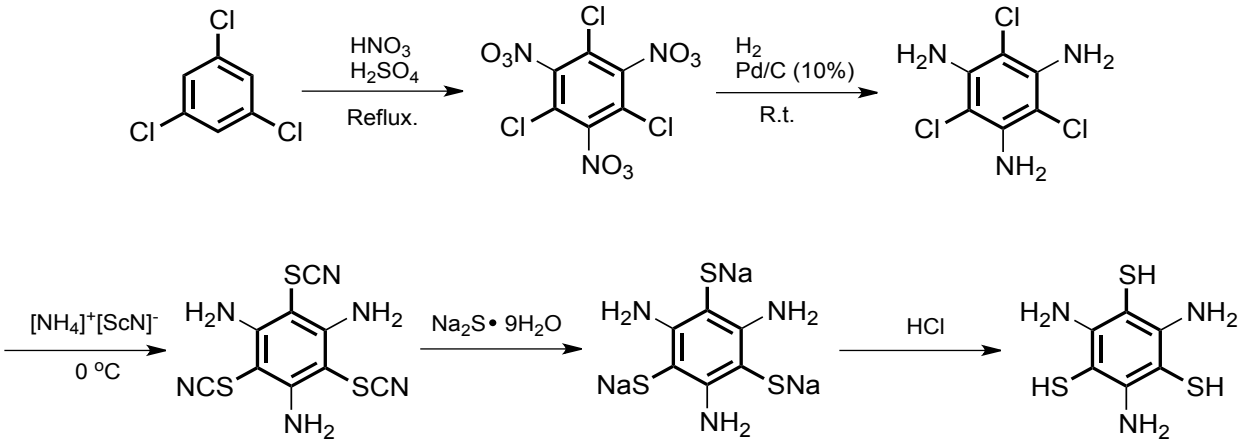

Fig. 2-4 | Schematic illustration of synthetic approach 1,3,5-Triaminobenzene-2,4,6-trithiol **(L1).**

Substrate preparation. HOPG was purchased from Alliance Biosystems, Inc. (Grade SPI-1 10 × 10 × 2 mm) and cleaved with adhesive tape prior to use. Silicon wafers (P-doped with a carrier concentration of 3×10^{18} cm^{-3}) with thermally-grown 100-nm-thick SiO_2 were purchased from Yamanaka Semiconductor and cut into squares (10 × 10 mm). 1,1,1,3,3,3-Hexamethyldisilanaze (HMDS)-modified SiO_2/Si substrates were prepared by depositing HMDS on SiO_2/Si substrates, keeping them under vacuum for 10 min, and then placing them in a flow of Ar. The HMDS-modified SiO_2/Si substrates were kept in anhydrous ethanol.

2-2-2 Synthesis

Preparation of bulk-NiIT. Under an argon atmosphere, a degassed aqueous solution (10 mL) containing 1,3,5-triaminobenzene-2,4,6-trithiol **(L1)** (5 mM) and $FcBF_4$ (5 mM) was prepared. To this solution, a solution of $Ni(OAc)_2 \cdot 6H_2O$ (2.5 mM) in 10 mL of 2.5 M aqueous ammonia was added dropwise with stirring. Stood in Ar atmosphere for an additional 1 hour, the solution became colorless, and the black precipitate (**bulk-NiIT**) was collected by filtration. **Bulk-NiIT** was thoroughly washed with water and ethatnol, and dried *in vacuo* for 12 hours.

Preparation of nano-NiIT. Under an argon atmosphere, degassed dichloromethane (5 mL) containing $Ni(acac)_2$ (0.5 mM) was placed in a glass vial with a diameter of 40 mm, to prepare a saturated solution. The dichloromethane solution was covered with degassed water (5 mL) to form a double layer. A degassed aqueous solution (5 mL) containing 2.4×10^{-5} mol L^{-1} of **L**, $FcBF_4$, and aqueous ammonia was added to the water phase. After 7 days, multi-layer **nano-NiIT** emerged at the interface as a brown film. After the removal of the aqueous and organic phases, multi-layer **nano-NiIT** was washed thoroughly with water, ethanol, and dichloromethane, and dried *in vacuo* at 120 °C. **nano-NiIT** is stable under air, can tolerate the heat till 200 °C.

2-2-3 Instrument and characterization methods

Characterization. Optical microscope images were taken using VHX-100 (Keyence Corporation). FE-SEM images were collected using a scanning electron microscope (JSM-7400 FNT, JEOL). The samples were prepared by depositing an ethanol suspension of **nano-1** on HMDS-modified SiO_2/Si substrates. TEM images were recorded with a transmission electron microscope (HF-2000, Hitachi) equipped with a AMT-CCD camera (HISCO, AMT552) at 75 keV. The TEM samples were prepared by depositing an ethanol suspension of **nano-1** on a carbon film supported by a copper grid. ATR-IR spectra were recorded using an IR spectrometer (FT/IR-6100, JASCO) at room temperature under vacuum. The samples were prepared by depositing **bulk-NiIT, NiIT-M, L1 and nano-NiIT** on HMDS-modified SiO_2/Si substrates. XPS data were obtained using an XPS microprobe (PHI 5000 VersaProbe, ULVAC-PHI, Inc.). Al Kα (15 kV, 25 W of 1456 eV) was used as the X-ray source, and the beam was focused on a 100 μm^2 area. The spectra were analyzed with MultiPak (MultiPak Version 9.2.0.5 ULVAC-PHI, Inc.), and standardized using the C (1s)

peak at 284.8 eV. Atomic force microscopy measurements were carried out using a scanning probe microscope (5500, Agilent Technologies) under ambient conditions high-amplitude mode (tapping mode) with a silicon cantilever probe (PPP-NCL, Nano World).

SAED simulation. To analyze the obtained SAED pattern (Figure 3e), the atomic arrangement of single-layer **nano-NiIT** was optimized using density-functional theory implemented in performed on Gaussian 09:[28] All the optimized structures were obtained at the B3LYP level of theory. As the basis sets, 6-31G* is used. The optimized cell was then subjected so as to reproduce the observed diffraction data. The eclipsed and staggered stack models were then constructed by using space group of P_6/mmm and P_{63}/mmc, respectively. The SAED patterns were simulated by implementing CrystalMaker 2.6.3, SingleCrystal 2.3, and CrystalDiffract 6.5.5 (CrystalMaker Software Ltd).

2-3 Results and discussion

2-3-1 Single-phase synthesis of bulk-NiIT

To confirm the multinuclear coordination ability, a bulk material **bulk-NiIT** was synthesised in a homogeneous system as follows. Under an argon atmosphere, **L1** and an oxidising agent, ferrocenium tetrafluoroborate ($FcBF_4$) were dissolved in water to prepare a saturated solution. $FcBF_4$ was employed because ferrocenium ion is effective to oxidise bis(aminobenzenethiolato)nickel to bis(iminobenzenethiolato)nickel.[33] To this solution, $Ni(OAc)_2$ dissolved in aqueous ammonia was added dropwise with stirring. A black precipitate was formed immediately. After standing the solution under argon for 1 h, the black precipitate (**bulk-NiIT**) was collected by filtration (Fig. 2-5). Insoluble **bulk-NiIT** was thoroughly washed with water, ethanol and acetone, and dried under vacuum.

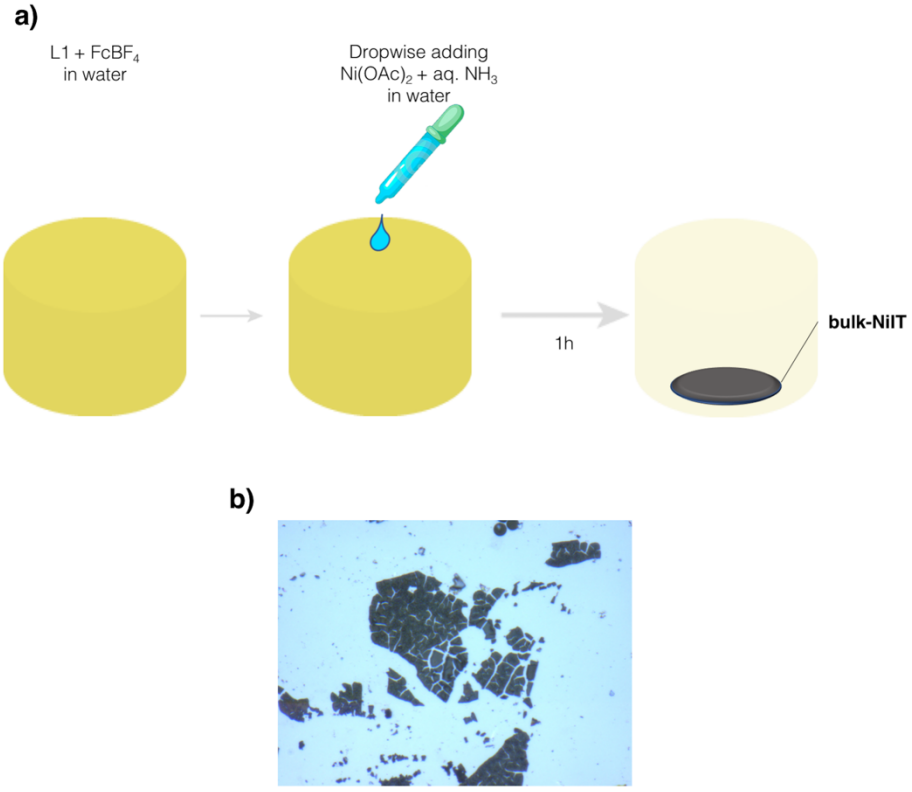

Fig. 2-5 | Single-phase syntheses of **bulk-NiIT**. **a**) Schematic illustration of the syntheses. **b**) Photographs of powdery **bulk-NiIT** drop casted on silicon substrate.

2-3-2 Chemical compositions of bulk-NiIT

The elemental composition and chemical bonding of **bulk-NiIT** were investigated by X-ray photoelectron spectroscopy (XPS), and infrared (IR) spectroscopy. XPS spectra are, for the most part, quantified in terms of peak intensities and peak positions. The peak intensities measure how much of a material is at the surface, while the peak positions indicate the elemental and chemical composition. XPS of **bulk-NiIT** placed on highly oriented pyrolytic graphite (HOPG) to evaluate its component elements detected N, S, and Ni with the ratio of 40.1 : 39.4 : 19.3 by comparing peaks intensity, which is approximately compatible with the theoretical value of 2 : 2 : 1, intimating the quantitative generation of bis(iminothiolato)nickel units in the bulk material (Fig. 2-6). For reference, **L1** on silicon substrate and a neutral mononuclear complex, bis(1-iminobenzene-2-thiolato) nickel(II), **NiIT-M**,[27] deposited on HOPG were subjected to XPS (Fig. 2-7 and Fig. 2-8). **L1** did not show any Ni 2p peak, while the peak was present at alike binding energy in **NiIT-M** (Fig. 2-8 b) to **bulk-NiIT** (Fig. 2-6 b). High-resolution XPS can differentiate the chemical environment of an element. The binding energy of the N 1s signal for **bulk-NiIT** (400.0 eV) was indistinguishable to that in **NiIT-M** (399.9 eV, Fig. 2-8 c), attributable to nitrogen in the imino-Ni binding state (Fig. 2-6 b).18 The S 2s peak was exhibited at 227.6 eV (Fig. 2-6 d), which is also consistent with that at **NiIT-M** (Fig. 2-7 c). These results indicate that the oxidation state of complex in **bulk-NiIT** is neutral.

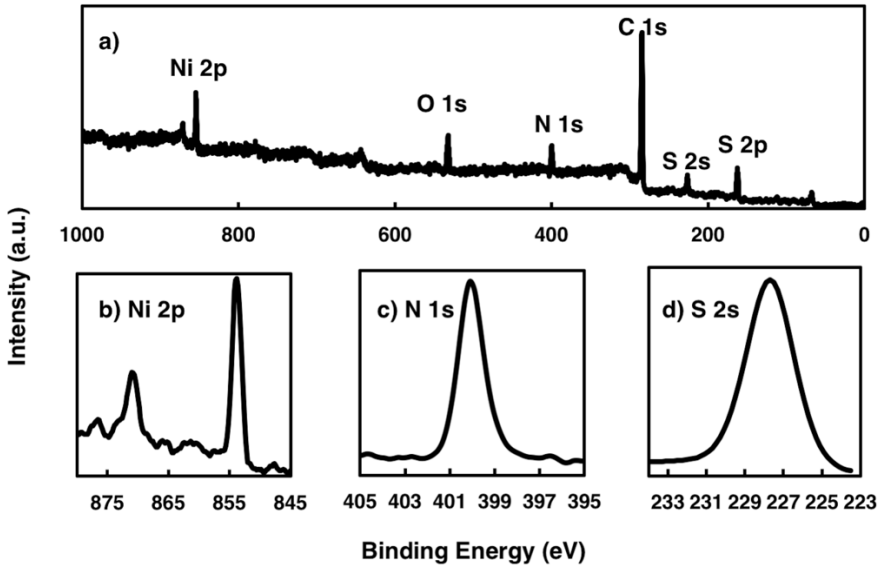

Fig. 2-6 | XPS of **bulk-NiIT**. **a)** Wide-scan XPS of ligand **bulk-NiIT. b)** Narrow-scan XPS of **bulk-NiIT** focusing on the Ni 2p region; **c)** the N 1s region; **d)** the S 2s region.

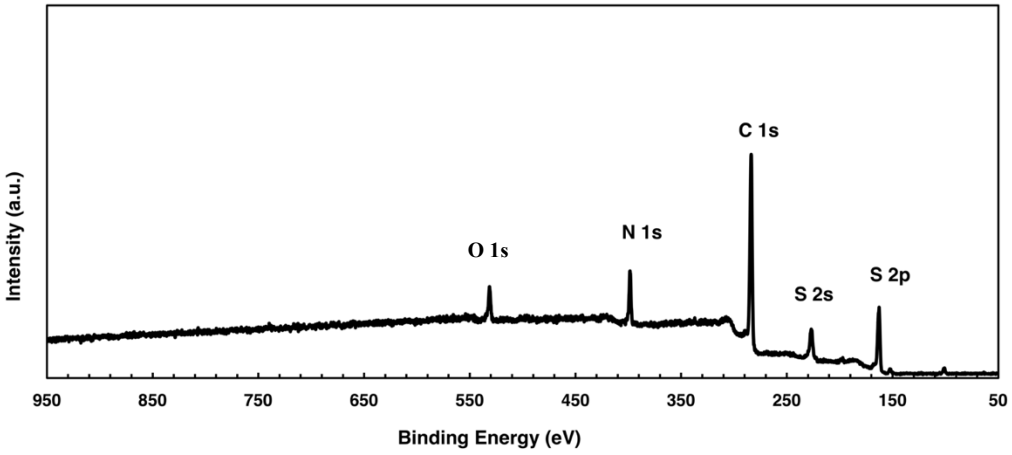

Fig. 2-7 | Wide-scan XPS of ligand **L1.**

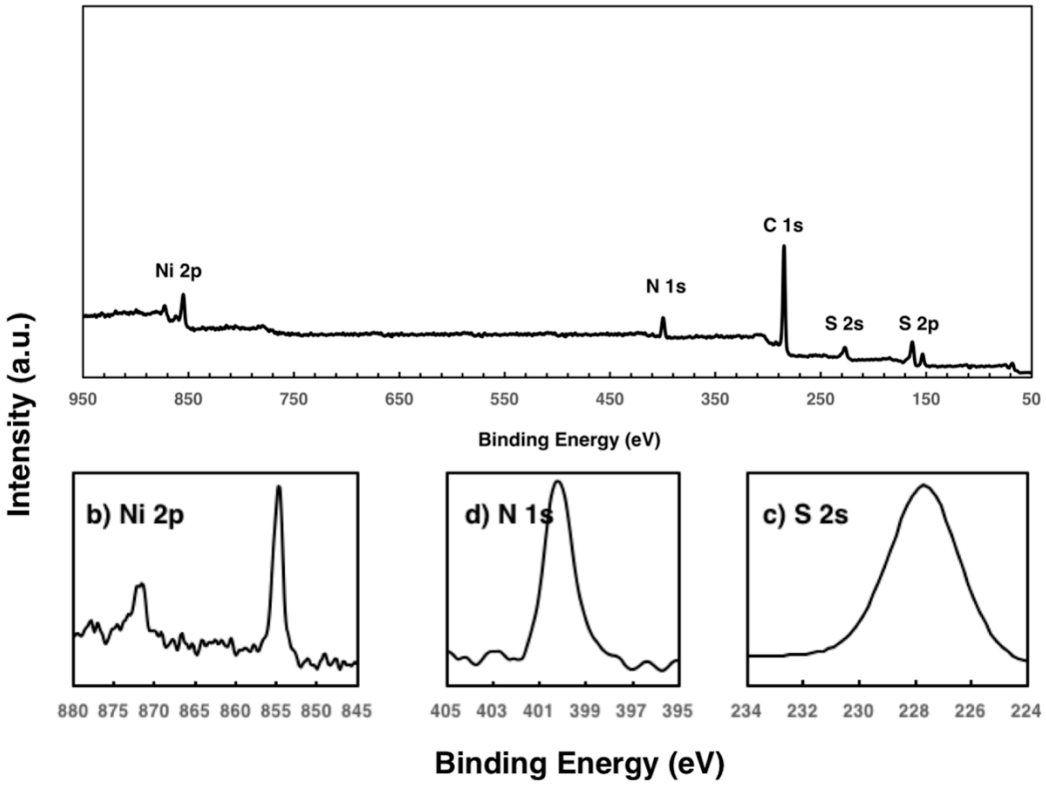

Fig. 2-8 | XPS of **NiIT-M. a)** Wide-scan XPS of mononuclear **NiIT-M**. Narrow-scan XPS focusing on **b)** the Ni 2p region, **c)** the N 1s region, **d)** the S 2s region.

Figure 2-9 explains IR spectra of **bulk-NiIT** obtained using the ATR method. There is no S−H stretching vibration signal around 2500 cm^{-1}, while this signal was recognised for **L1** (Fig. 2-9 a), indicating that all the thiol groups of **L1** have associated in coordinating to the Ni centre.[23] Whereas the amino groups in **L1** display two bands at 3325 cm^{-1} and 3390 cm^{-1} attributed to antisymmetric N-H stretching, **bulk-NiIT** features one band at 3286 cm^{-1}. This determination indicates that not the amino group but the imino group coordinates to the Ni centre, which is compatible with the reaction mechanism of oxidation accompanied by deprotonation (Fig. 2-9 b).

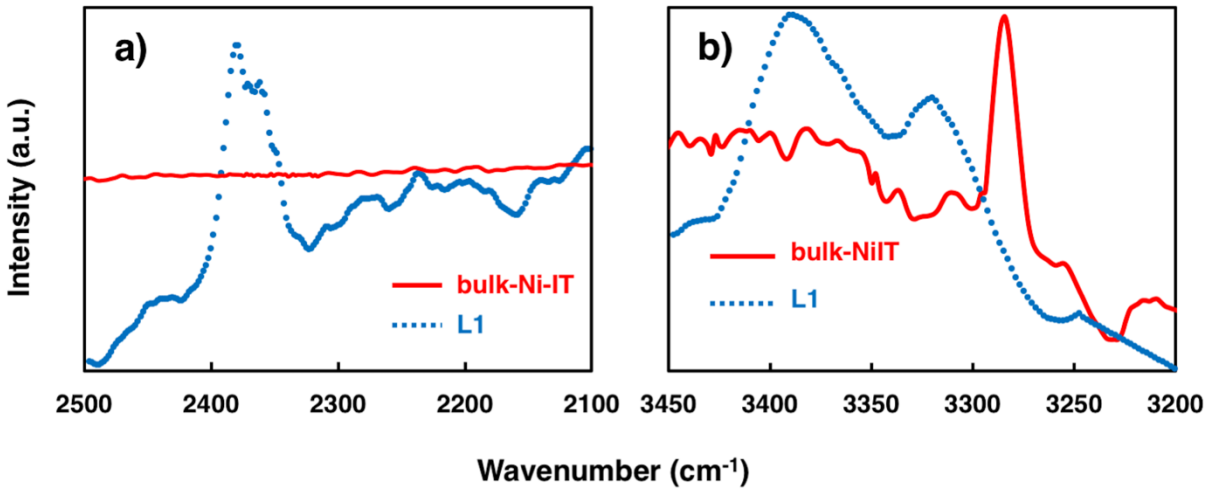

Fig. 2-9 | IR spectra of **bulk-NiIT** and **L1**: **a)** in the S-H stretching vibration region; **b)** in the N-H stretching vibration region.

2-3-3 Microscopic observation of bulk-NiIT

I studied the structure of **bulk-NiIT** by drop casting **bulk-NiI**T with ethanol on Si(111) substrate, subjected for field-emission scanning electron microscopy (FE-SEM). Most of the material settled as 3D clumps, and this behaviour could be ascribed to stochastic coordination between the two components (**L1** and Ni^{2+}), forming miss-orientation among the layers. However, interestingly, some fragments express characters indicating 2D packing properties (Fig. 2-10 a, b); the peeled-off part of material shows applanation pieces, while the halting section exhibits a stair-like pattern; furthermore, the edge of substance appears as layered morphology (Fig. 2-10 b). These arrangements hint that **bulk-NiIT** could be comprised of 2D-planary formations randomly aggregated to each other.

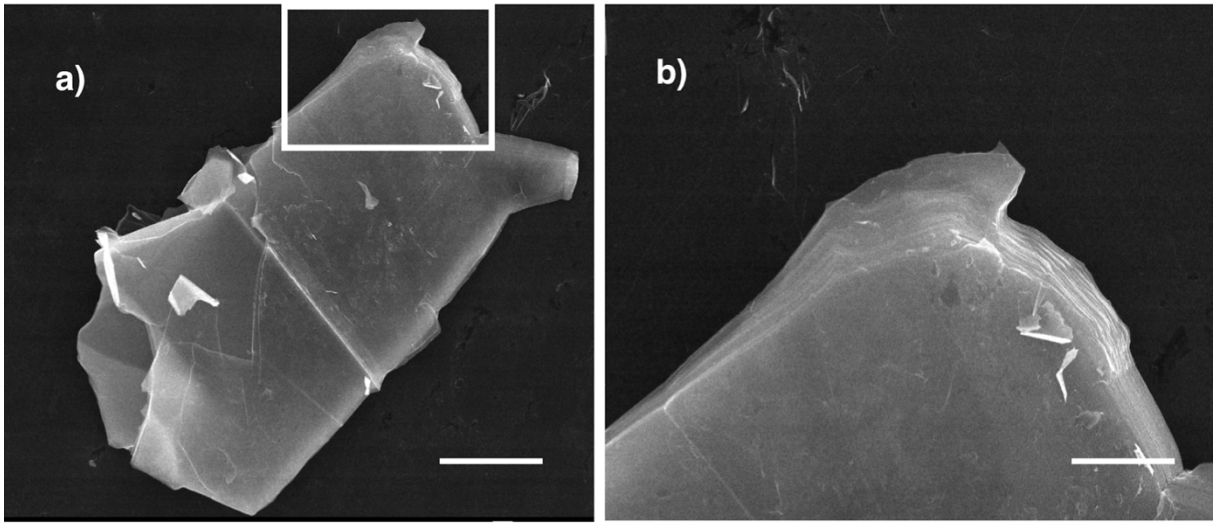

Fig. 2-10 | a) FE-SEM images on HMDS/ Si(111) of **bulk-NiIT**; **b)** and its magnification of rectangular area. Scale bars represent 2 μm for **a**, and 500 nm for **b**.

2-3-4 Liquid/liquid interfacial synthesis of nano-NiIT

After confirming the coordination feasibility, I move to the fabrication of two-dimensional material as the next step. The liquid-liquid interface was used to manufacture a filmy structure of **NiIT**.[23] When an aqueous solution of **L1**, $FcBF_4$ and aqueous ammonia was gently set on top of a dichloromethane solution of bis(2,4-pentanedionato)nickel(II) ($Ni(acac)_2$). Then, the bilayer system was set under argon at room temperature for five days. A flat sheet-like **nano-NiIT** was developed at the liquid-liquid interface. The as-prepared **nano-NiIT** was cleaned by substituting each layer of the solution with pure solvent. After eliminating the upper aqueous layer carefully, it was transferred onto planar substrates such as 1,1,1,3,3,3-hexamethyldisilazane-modified silicon(111) [HMDS/Si(111)].

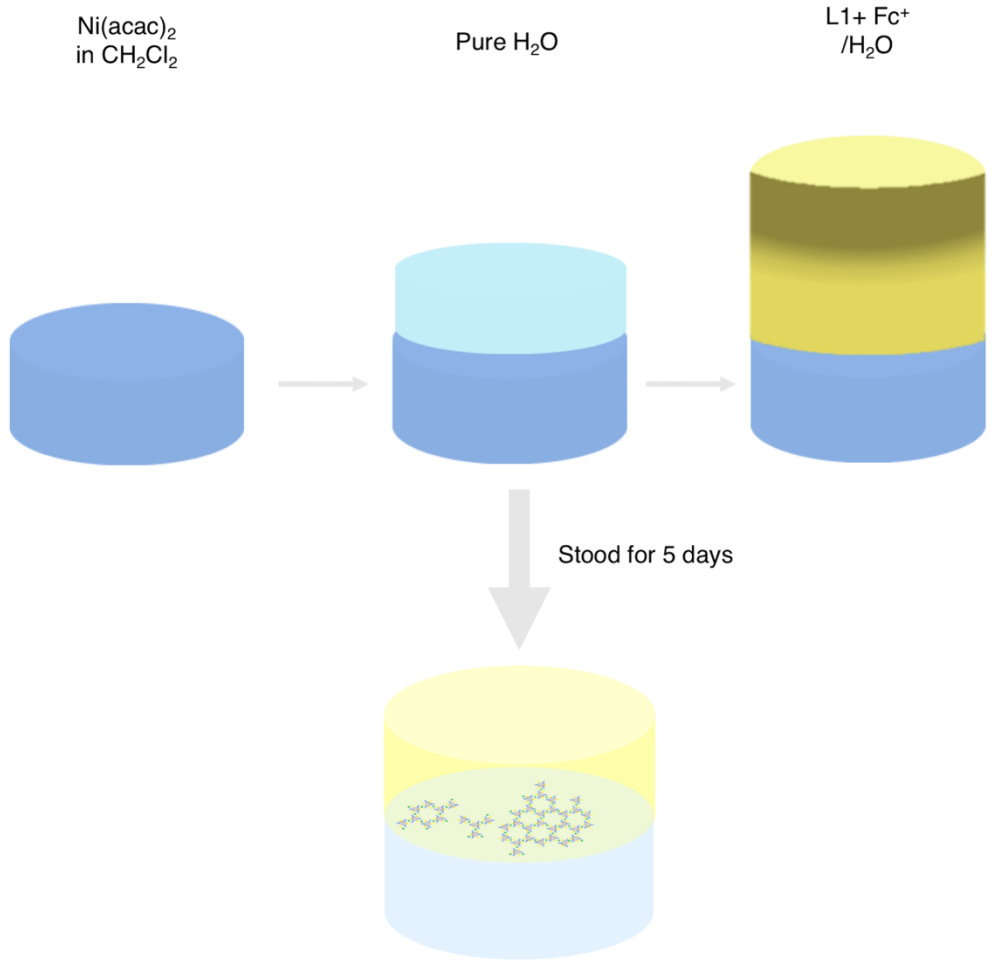

Fig. 2-11 | Liquid-liquid interfacial syntheses of **nano-NiIT**.

2-3-5 Microscopic observation of nano-NiIT

Optical microscopy of the **nano-NiIT** generated by the liquid/liquid interfacial synthesis disclosed a flat, uniform film like morphology with a presence of cracks and wrinkles (Fig. 2-12). FE-SEM reveals also a flat, uniform film with the size over 10 μm (Fig. 2-13).

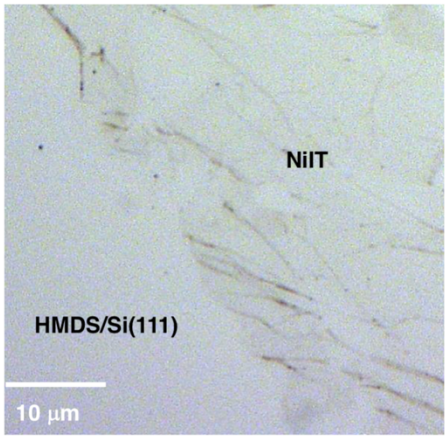

Fig. 2-12 | Optical microscope of **nano-NiIT** on HMDS/ Si(111).

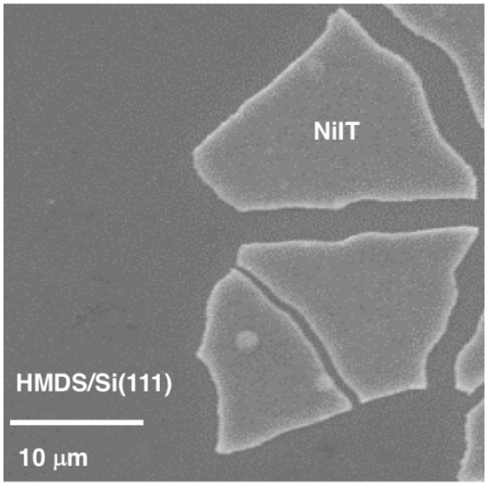

Fig. 2-13 | FE-SEM images on HMDS/ Si(111) of **nano-NiIT**.

Atomic force microscopy (AFM) identifies the intermolecular force between a tip and a CONASH exterior. The force feedback data are then consolidated into a 3D topographic representation. Usually, a nanosheet sample is immobilised on a planar substrate to allow continuous measurements. Its accurate interpretation and high sensitivity make AFM critical for describing the morphology of material and defining its thickness and domain size. An AFM image of **nano- NiIT** is presented in Fig. 2-14, where a flat and thin film with thickness of 20 nm over 5 μm × 15 μm area is displayed. As the thickness of a single layer would be ca. 0.6 nm based on the analogy to the bis(ditholato)nickel nanosheet,[23] the film consists of around 30 layers. Some wrinkles were thoroughly distributed on the sheet, which is main cause for the roughness for topography cross-section analysis, but this reveals the nature of **nano-NiIT** to be a uniform, flexible cloth-like morphology.

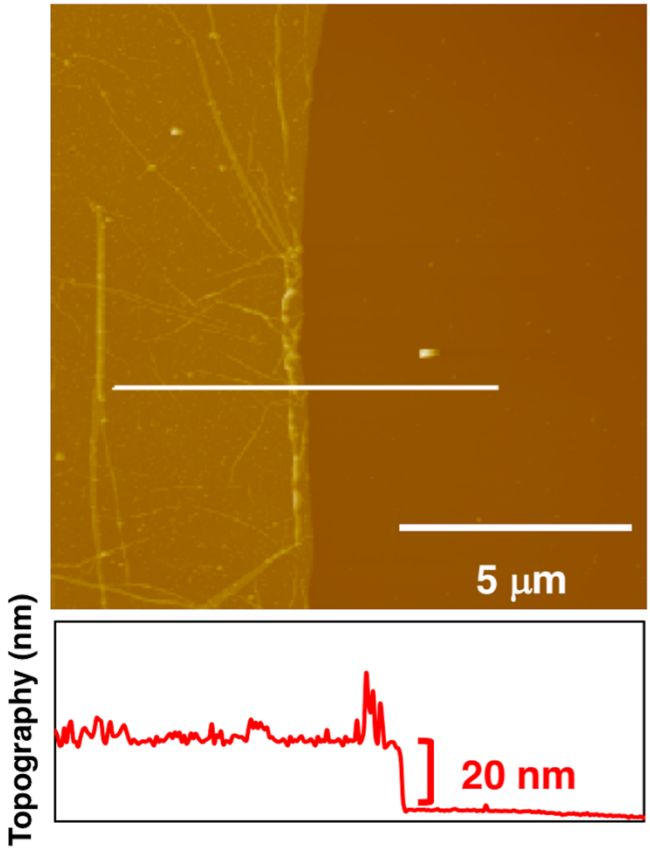

Fig. 2-14 | AFM image of **nano-NiIT** on HMDS/Si(111) and its cross-section analysis along the magenta line of multilayer of **nano-NiIT**.

Gas–liquid interfacial synthesis was difficult for producing single-layered **nano-NiIT** due to rapid aggregation; however, by decreasing the concentrations of **L1** and $Ni(acac)_2$ salt to 1/200 and 1/50, respectively, of their original concentrations in the liquid–liquid interfacial synthesis, few-layered **nano-NiIT** 10 nm thick was produced.

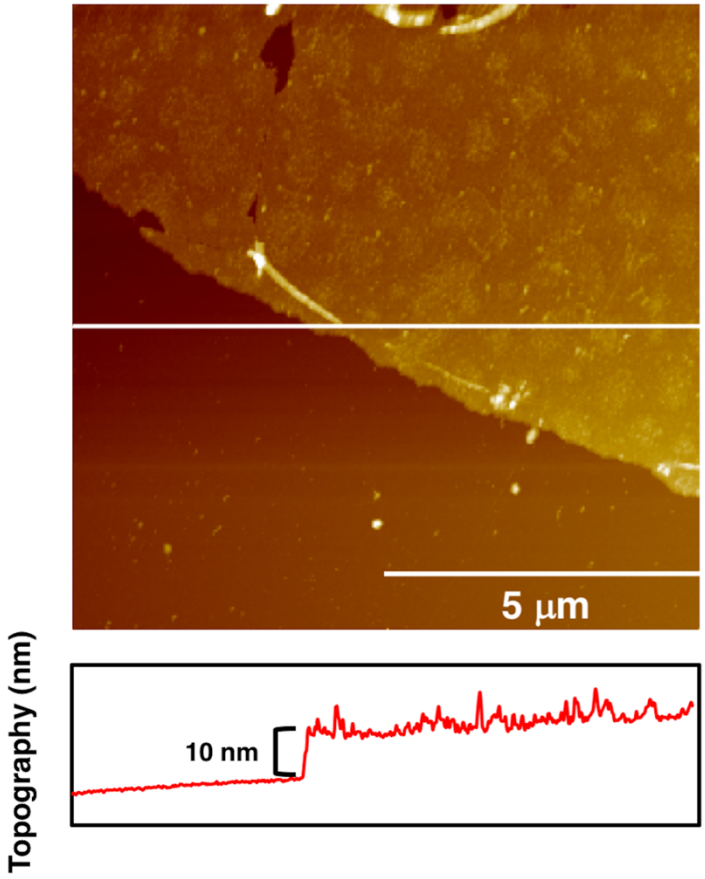

Fig. 2-15 | AFM image of **nano-NiIT** on HMDS/Si(111) and its cross-section analysis along the magenta line of few-layer **nano-NiIT**.

High-resolution transmission electron microscopy (HR-TEM) showed **nano-NiIT** to have a pile morphology (Fig. 2-16 a), suggesting a layered structure. Selected-area electron diffraction (SAED) gave a hexagonal pattern (Fig. 2-16 b), presenting d-spacing of 0.203 nm with in-plane 0 6 0 diffraction. The simplified ring structured model correlated to **NiIT** systems suggest that **NiIT** have a hexagonal lattice with cell lengths of 1.405 nm (Fig. 2-17 a). The diffraction pattern in figure 2-16 b is consistent with in-plane diffraction patterns reproduced from crystal lattices containing piles of single-layer **nano-NiIT** (Fig. 2-17 b). Although this index number is considerably big, its reciprocal space d-spacing agrees with the multiple of its 0 1 0 diffraction reciprocal d-spacing. Moreover, similar 0 6 0 diffraction was observed in our group's previous study on an isoelectronic bis(dithiolato)nickel nanosheet.[23] This result expresses that **nano-NiIT** was crystalline in nature with a hexagonal lattice.

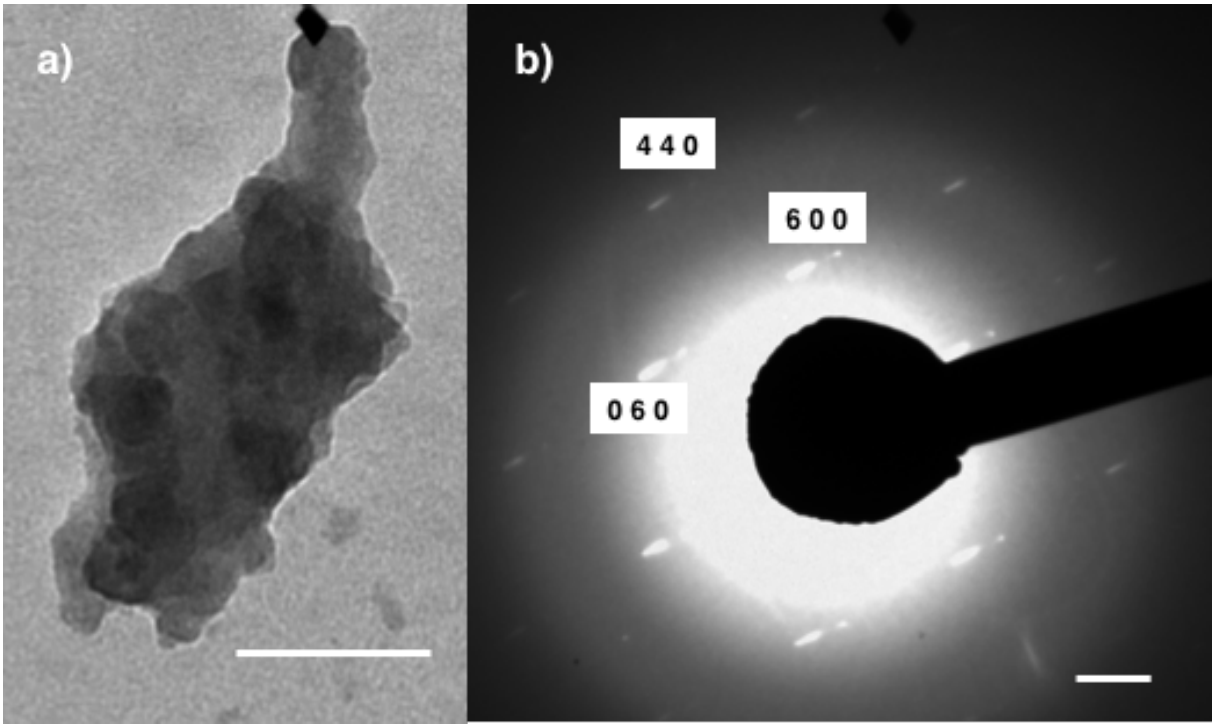

Fig. 2-16 | a) HR-TEM of **nano-NiIT**. Scale bars represent 500 nm. **b)** SAED pattern of nano-NiIT. Scale bar represents 2 nm^{-1}.

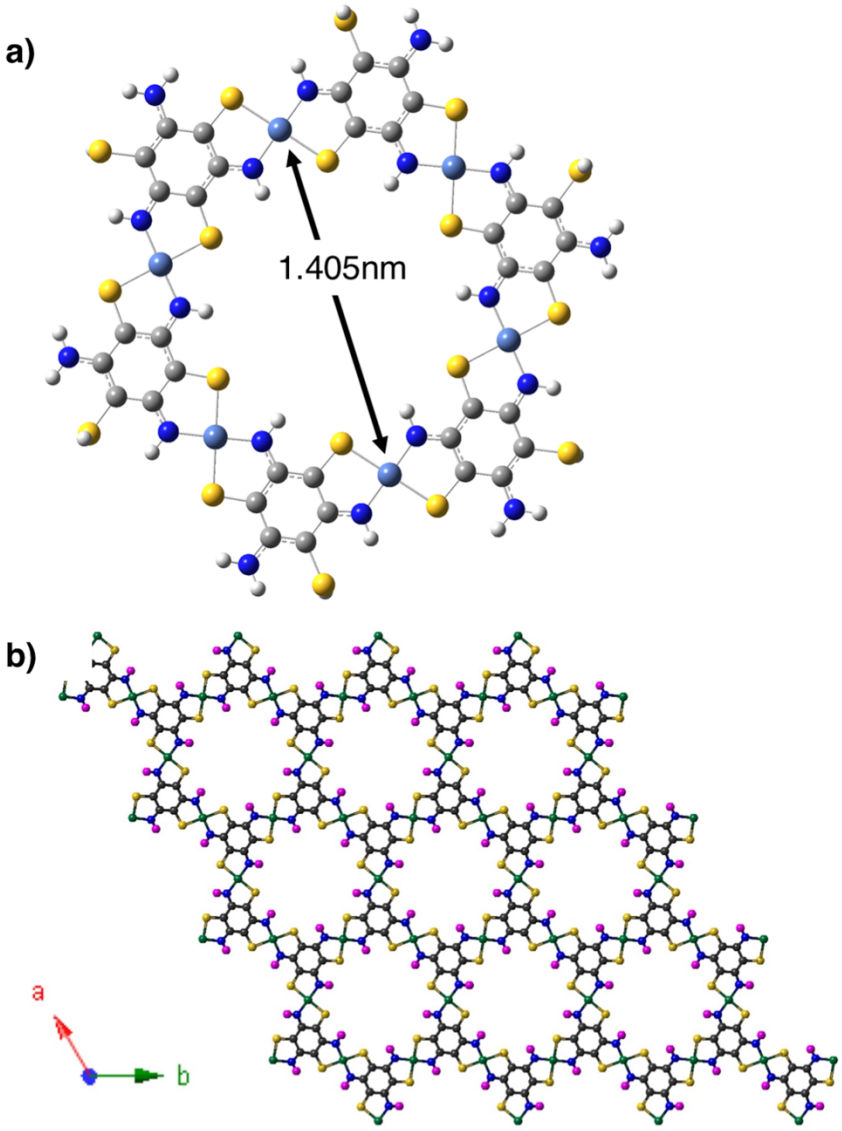

Fig. 2-17 | a) Gaussian simulation results of simplified ring model of **NiIT**. **b)** Simulations of monolayer of **NiIT**.

2-3-6 Chemical compositions of nano-NiIT

XPS and IR characterization of **nano-NiIT** unveiled agreement with **bulk-NiIT**. XPS of **nano-NiIT** showed the abundance ratio of N: S: Ni is 36.9: 41.3: 21.7, which is nearly consistent with the ideal value of N: S: Ni = 2: 2: 1. These conclusions indicate that the nickel(II) iminothiolato complex motif developed quantitatively in the nanosheet (Fig. 2-18). The spectrum of **nano-NiIT** features N 1s peaks at the binding energy of 399.9 eV (Fig. 2-18 c) and the S 2s peak at 227.4 eV (Fig. 2-18 d), which concur with the results of **bulk-NiIT**.

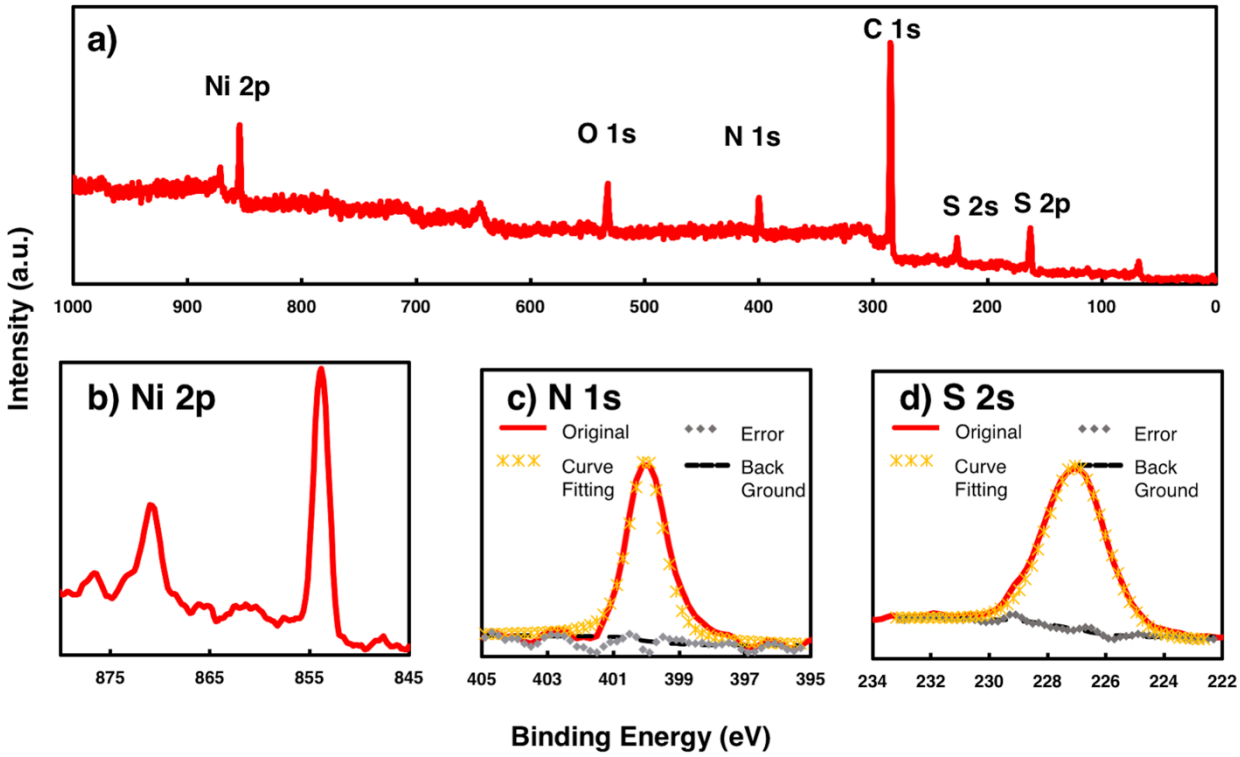

Fig. 2-18 | XPS of **nano-NiIT. a)** Wide-scan XPS of **nano-NiIT**. Narrow-scan XPS focusing on **b)** the Ni 2p region; **c)** the N 1s region; **d)** the S 2s region.

ATR-IR spectra **of nano-NiIT** exhibited no trace of S–H stretching vibration at ~2500 cm^{-1}, implying that all thiol groups in L participated in coordinating to the Ni centre. The signals for N-H stretching are very consistent to **bulk-NiIT** (Fig. 19), indicating the existence of imino moieties. Therefore, the spectroscopic analyses confirmed that **nano-NiIT** dwells the bis(iminothiolato)nickel moiety.

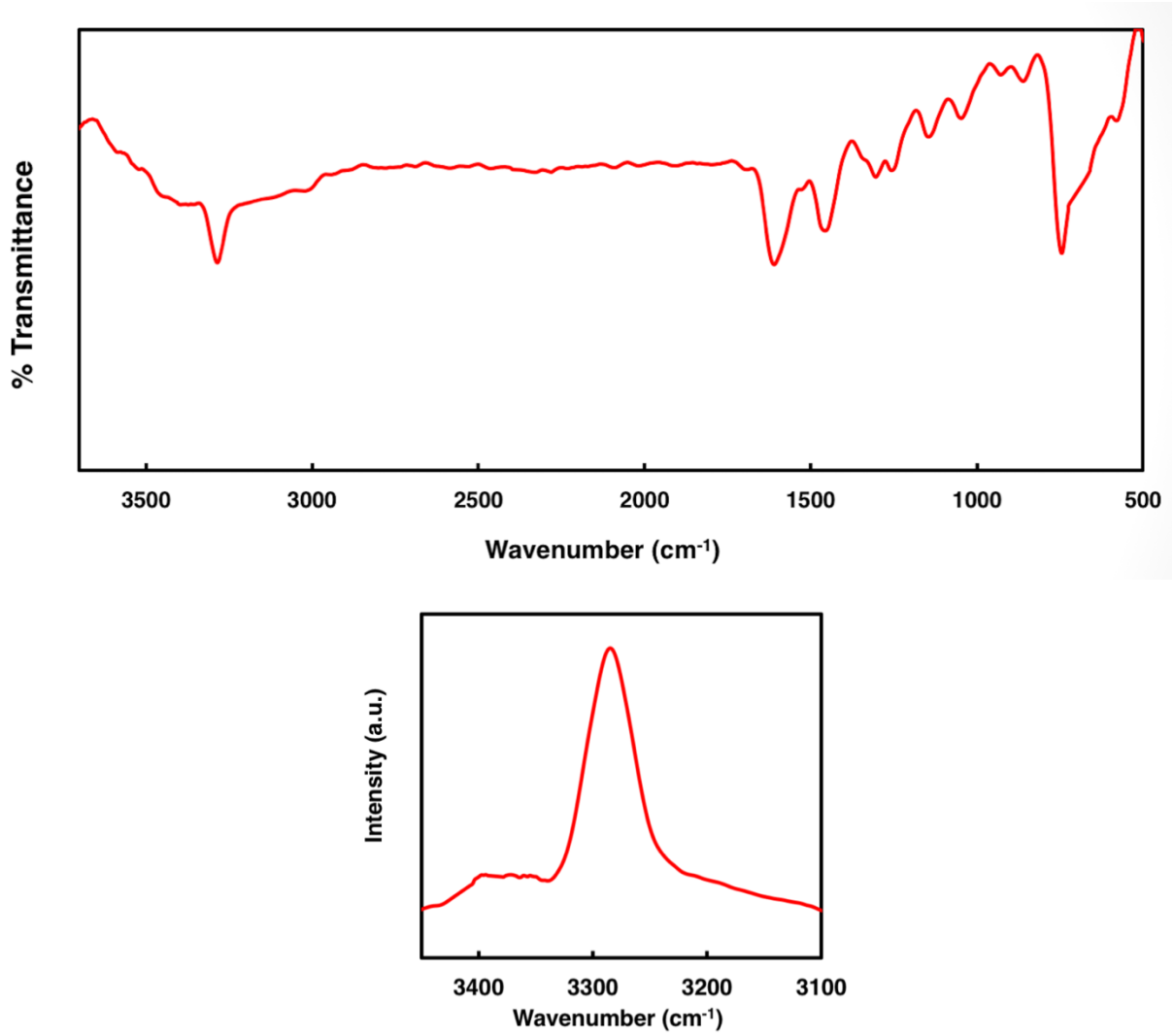

Fig. 2-19 | IR spectra of **nano-NiIT** and its N-H stretching vibration region.

2-3-6 Electroconductivity studies of nano-NIIT

Conclusively, motivated by the structural similarity of **NiIT** to bis(dithiolato)nickel and high electronic conductivity of bis(dithiolato)nickel nanosheet, we examined the electrical characteristics of **nano-NiIT**. The electrical conductivity of pelletized **nano-NiIT** was contained by the van der Pauw method to exclude the contact resistance between the sample and the probe. **Nano-NiIT** reveals the temperature dependent conductance down to 50 K from room temperature, indicated the semiconductive nature of the activation energy of 41 meV (Fig. 2-20 d). At 298 K, **nano-NiIT** showed an electrical conductivity of 1×10^{-1} S cm^{-1}, which is lower than the bis(dithilato)nickel nanosheet (160 S cm^{-1})[24] but higher than the bis(diimino)nickel nanosheet.[25] The dependence of conductivity on the isoelectronic chemical structures is attractive while the quantitative comparison of the intrinsic conductivity between **NiIT** nanosheet with that of bis(dithiolato)nickel nanosheet is difficult at this stage because the latter was measured not for the pelletized substance but for the filmy one.

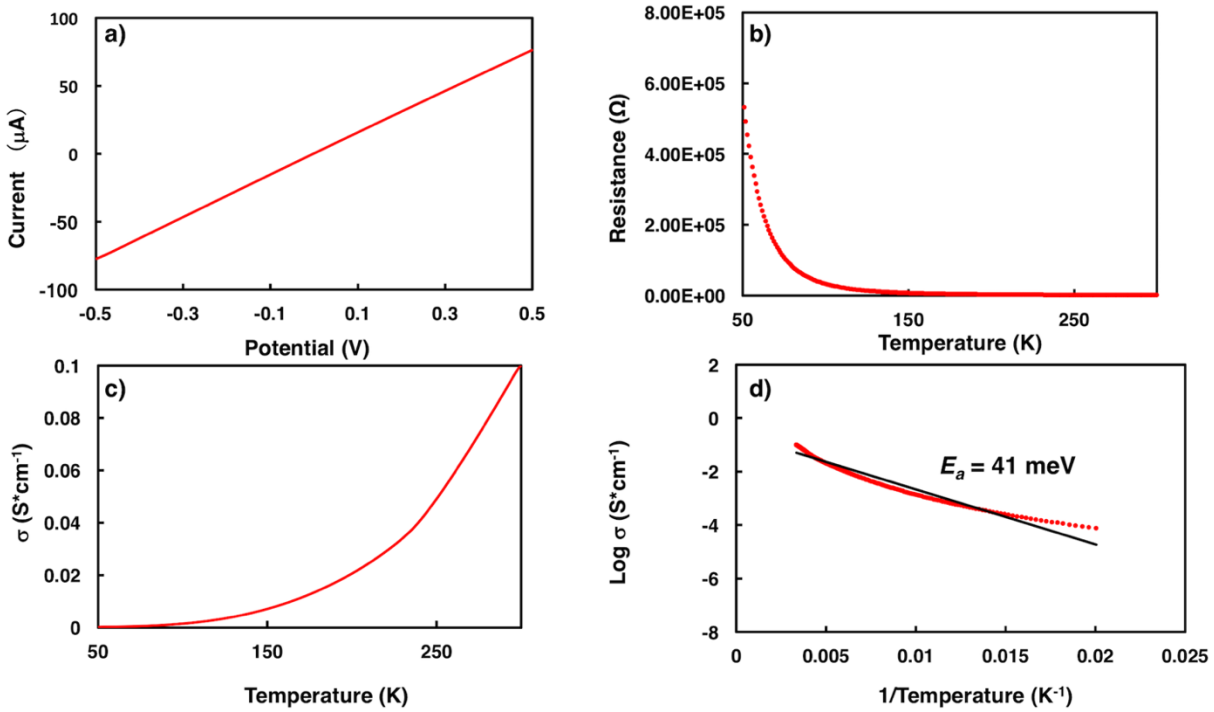

Fig. 2-20 | a) IV plot of **nano-NiIT**. **b**) Temperature depended resistance plot of **nano-NiIT. c**) **d**) Temperature depended conductivity plot of **nano-NiIT.**

2-4 Conclusion

In conclusion, a new π-conjugated CONASH comprised of S and NH mixed ligating group, **NiIT** was fabricated in both homogeneous and interfacial operations. A bulk material **bulk-NiIT**, which was fabricated by a single-phase homogenous reaction and characterised by XPS, IR and SEM, is composed of 2D-planary structures with a neutral bis(imonothiolato)nickel(II) motif randomly aggregated to each other. A thin film, **nano-NiIT** was synthesised by the liquid/liquid interfacial coordination reaction. The morphology, composition, and lattice structure of the complexes were investigated by SEM, AFM, XPS, IR and HR-TEM. **Nano-NiIT** exhibited an electrical conductivity of 1×10^{-1} S cm^{-1} at room temprature with the semiconductive nature. This successful fabrication of a new π-conjugated nanosheet, **nano-NiIT**, will further expand the diversity of researches in the field of coordination two-dimensional material.

2-5 References

1 C. Joachim, J. K. Gimzewski and A. Aviram, *Nature,* 2000, **408**, 541.

2 J. Park, A. N. Pasupathy, J. I. Goldsmith, C. Chang, Y. Yaish, J. R. Petta, M. Rinkoski, J. P. Sethna, H. D. Abruña, P. L. McEuen and D. C. Ralph, *Nature*, 2002, **417**, 722.

3 C. E. D. Chidsey and R. W. Murray, *Science*, 1986, **231**,25

4 I. M. Piglosiewicz, R. Beckhaus, G. Wittstock, W. Saak and D. Haase, *Inorg. Chem.*, 2007, **46**, 7610.

5 T. Weyland, K. Costuas, L. Toupet, J.-F. Halet and C. Lapinte, *Organometallics*, 2000, **19**, 4228.

6 R. Modak, Y. Sikdar, S. Mandal and S. Goswami, *Inorg. Chem. Commun.*, 2013, **37**, 193.

7 S. Ohta, S. Yokozawa, Y. Ohki and K. Tatsumi, *Inorg. Chem.*, 2012, **51**, 2645.

8 M. Rivera-Carrillo, I. Chakraborty, G. Mezei, R. D. Webster, R. G. Raptis, *Inorg. Chem.*, 2008, **47**, 7644.

9 J. E. Perea-Buceta, A. J. Mota, J.-P. Costes, R. Sillanpää, J. Krzystek and E. Colacio *Dalton Trans.*, 2010, **39**, 10286.

10 A. Figuerola, V. Tangoulis, J. Ribas, H. Hartl, I. Brudgam, M. Maestro, C. Diaz, *Inorg. Chem.*, 2007, **46**, 11017.

11 L. M. Mirica and T. D. P. Stack *Inorg. Chem.*, 2005, **44**, 2131.

12 J. Yoon, L. M. Mirica, T. D. P. Stack and E. I. Solomon, *J. Am. Chem. Soc.*, 2004, **126**, 12586.

13 S. Ferrer, F. Lloret, I. Bertomeu, G. Alzuet, J. Borras, S. Garcia-Granda, M. Liu-Gonzalez and J. G. Haasnoot, *Inorg. Chem.*, 2002, **41**, 5821.

14 J. Yoon, L. M. Mirica, T. D. P. Stack and E. I. Solomon, *J. Am. Chem. Soc.*, 2004, **126**, 12586-12595.

15 C. P. Raptopoulou, V. Tangoulis and V. Psycharis, *Inorg. Chem.*, 2000, **39**, 4452.

16 J. K. Gardner, N. Pariyadath, J. L. Corbin and E. I. Stiefel, *Inorg. Chem.*, 1978, **17**, 897.

17 M. Ebadi and A. B. P. Lever, *Inorg. Chem.*, 1999, **38**, 467.

18 D. Sellmann, S. Emig, F. W. Heinemann and F. Knoch, *Angew. Chem.*, 1997, **109**,

1250; *Angew. Chem., Int. Ed. Engl.*, 1997, **36**, 1201.

19 D. Herebian, E. Bothe, E. Bill, T. Weyhermüller, and K. Weighardt, *J. Am. Chem. Soc.*, 2001, **123**, 10012.

20 E. K. Beloglazkina, A. A. Moiseeva, A. V. Churakov, I. S. Orlov, N. V. Zyk, J. A. K. Howard and K. P. Butin, *Russ. Chem. Bull.*, 2002, **51**, 467.

21 K. Ray, T. Weyhermüller, F. Neese and K. Wieghardt, *Inorg. Chem.*, 2005, **44**, 5345.

22 S. Noro, T. Takenobu, Y. Iwasa, H.-C. Chang, S. Kitagawa, T. Akutagawa and T. Nakamura, *Adv. Mater.*, 2008, **20**, 3399.

23 T. Kambe, R. Sakamoto, K. Hoshiko, K. Takada, M. Miyachi, J.-H. Ryu, S. Sasaki, J. Kim, K. Nakazato, M. Takata and H. Nishihara*, J. Am. Chem. Soc.*, 2013, **135**, 2462.

24 T. Kambe, R. Sakamoto, T. Kusamoto, T. Pal, N. Fukui, K. Hoshiko, T. Shimojima, Z. Wang, T. Hirahara, K. Ishizaka, S. Hasegawa, F. Liu and H. Nishihara, J. Am. Chem. Soc., 2014, **136**, 14357.

25 N. Lahiri, N. Lotfizadeh, R. Tsuchikawa, V. V. Deshpande and J. Louie, *J. Am. Chem. Soc.*, 2017, **139**, 19.

26 G. Grandolini, A. Martani and *Gazz. Chim. Ital.*, 1962, **92**, 1150.

27 A. Das, Z. Han, W. W. Brennessel, P. L. Holland, R. Eisenberg, *ACS Catal.*, 2015, **5,** 1397.

28 Gaussian 09, Revision B.01, M. J. Frisch et al. Gaussian Inc., Wallingford CT, **2010**.

Chapter 3 π-Conjugated Bis(aminothiolato)nickel Nanosheet

(This chapter is not published because it is scheduled to be published in journals or other publications within five years.)

Chapter 4

Electronic and Electrochemical Applications of NiIT and NiAT

(This chapter is not published because it is scheduled to be published in journals or other publications within five years.)

Chapter 5

π-Conjugated Bis(iminophenolato)nickel Nanosheet

(This chapter is not published because it is scheduled to be published in journals or other publications within five years.)

Chapter 6

Concluding Remarks

Acknowledgement

First and foremost, thanks to the Almighty God of Chemistry, who gave me challenges, joys and ability to accomplish this research work.

I wish to express my profound sense of gratitude towards my principal supervisor, Prof. Hiroshi Nishihara, who enlightened my way with his valuable guidance, suggestions and continuous encouragement, during the research work and the preparation of this thesis. The opportunity he gave me to study in The University of Tokyo has been really fantastic.

I am also thankful to my associate supervisors, Dr. Ryota Sakamoto, Dr. Testuro Kusamoto, Dr. Kuo-Hui Wu and Dr. Hiroaki Maeda for their advices. They have been great helps for me to settle into a new environment at the initial, and keep helping me along the way of research and life.

Also Professor Sono Sasaki and Dr. Hiroyasu Masunaga are thanked for the PXRD and GIXD measurements. Sate of art facilities in SPring-8 really gave me a lot help of nanosheet structure studies.

My collaborators, Professor Feng Liu, Mr. Wei Jiang and Ms. Xiaojun Ni, in University of Utah gave me many different aspects from their physics point of view. I am very grateful to them.

I would also like to thank all group members in Nishihara laboratory for being great people to have worked alongside and for the great laughs and memories as part of the team. They maximized the happy atmosphere in our group!

I would also like to thank many researchers and staff involved with me at The University of Tokyo for their help and support during my research.

Lastly, I owe my family members an expression of my gratitude for their patience, understanding, support and encouragement during the completion of this research work. I am especially grateful to Jessie Du; thank you for seeing me through the ups and downs. You have been amazing!

[Publication related to the thesis]

1. "Conducting π-Conjugated Bis(iminothiolato)nickel Nanosheet", X. Sun, K.-H. Wu, R. Sakamoto, T. Kusamoto, H. Maeda, H. Nishihara, *Chemistry Letters* 2017, 8, 1081.
2. Bis(aminothiolato)nickel Nanosheet as a Redox Switch for Conductivity and an Electrocatalyst for the Hydrogen Evolution Reaction", X. Sun, K.-H. Wu, R. Sakamoto, T. Kusamoto, H. Maeda, X. Ni, W. Jiang, F. Liu, S. Sasaki, H. Masunaga, H. Nishihara, submitted.

[Publication not related to the thesis]

1. "The coordination nanosheet (CONASH)", R. Sakamoto, K. Takada, X. Sun, T. Pal, T. Tsukamoto, E. J. H. Phua, A. Rapakousiou, K. Hoshiko, H. Nishihara, *Coord. Chem. Rev.* **320-321**, 118-128 (2016).